

Processing of Oceansat-2 Ocean Colour Monitor Data using SeaDAS

Technical Report

Ocean Sciences Division
AOSG / ECSA
National Remote Sensing Centre
Indian Space Research Organisation
Hyderabad - 500 625

**NATIONAL REMOTE SENSING CENTRE
REPORT / DOCUMENT CONTROL SHEET**

1.	Security Classification	Unclassified			
2.	Distribution	A Soft and hard copy available in OSD			
3.	Report / Document version	(a) Issue no. 01	(b) Revision & Date	R01/ 2012	December
4.	Report / Document Type	Technical Report			
5.	Document Control Number	NRSC/ECSA/AOSG/OSD/December-2012/TR-488			
6.	Title	Processing of Oceanst-2 Ocean Colour Monitor Data using SeaDAS			
7.	Particulars of collation	Pages 56	Figures 20	Tables 3	References 19
8.	Author(s)	T. D. Vara Prasad, T. Preethi Latha, K.H.Rao, S.B.Choudhury, P.V.Nagamani			
9.	Affiliation of authors	National Remote Sensing Centre			
10.	Scrutiny mechanism	Compiled by by OC Team	Reviewed by GD, AOSG	Approved /Controlled by DD, ECSA	
11.	Originating unit	Ocean Sciences Division, AOSG / ECSA			
12.	Sponsor(s) / Name and Address	NCP Project			
13.	Date of Initiation	February 2012			
14.	Date of Publication	December 2012			
15.	<p>Abstract (with Keywords): From this study we conclude that, Oceansat-2 Ocean Colour monitor being a global mission needs globally accepted geophysical data products. for this purpose we need to process OCM-2 data with uniform bio-optical algorithms, uniform atmospheric correction processed including flags, masks and other ancillary information which is globally accepted for the other Ocean Colour missions for generating the geophysical data products. Hence, we took an initiative to process OCM-2 data using the global ocean colour data processing software for generating the geophysical parameters. Apart from this the products generated by OCM-2 needs to be validated in both Indian as well as global waters for wide acceptance of OCM-2 products. Initially we validated OCM-2 data with three coastal cruises conducted in the Bay of Bengal in 2012.</p> <p>Key words: OCM-2, SeaDAS, LAC data, GAC data, binned products, validation</p>				

List of Contents

S.No	Content	Page No.
	Summary	
1	Introduction	1
2	Oceansat-2 Ocean Colour Monitor (OCM-2)	2
3	Visibility / Coverage of OCM-2 Sensor for LAC data Products	4
4	OCM-2 Data Products and their Representation	5
5	Processing of OCM-2 data using SeaDAS Software	7
6	Methodology	8
6.1	Atmospheric Correction	9
6.2	Concept of NIR Correction	10
6.3	Aerosol Model selection for Atmospheric Correction	11
6.4	Bio-optical Model for NIR Iteration	13
6.5	Spectral Dependency of the IOP's	14
6.5.1	Backscattering	14
6.5.2	Absorption	15
6.6	Iteration Method	16
6.7	Ancillary Data information	17
6.8	Flags, Masks and Thresholds	18
6.8.1	FLAGS	18
6.8.2	MASKS	18
6.9	Binning	19
7	Validation of OCM-2 chlorophyll with <i>in-situ</i> measurements	20
7.1	Validation in the Coastal Waters of Off Mahanadi and Paradip	20
7.2	Validation in the Coastal Waters of Godavari Basin	29
7.2.1	<i>In-situ</i> data processing	29
7.2.2	Study Area	30
7.3	Materials and Methods / Data Collection	31
7.3.1	Instruments Used - Hyperpro-II	31
7.3.2	Water Sample Collection	32
7.4	Data processing methods	33
7.4.1	<i>In-situ</i> data processing	33
7.4.2	High Performance Liquid Chromatography Analysis	33
7.5	Results and Analysis	34
7.5.1	Comparison of <i>in-situ</i> chlorophyll-a with OCM-2	34
7.5.2	Comparison of <i>in-situ</i> (radiometer) chlorophyll-a with HPLC	35
7.5.3	Comparison of HPLC chlorophyll-a with OCM2	36
7.5.4	Inferences	36
8	Conclusions	39
9	Acknowledgements	39
10	References	39
	Annexure-I	42
	Annexure-II	43
	Annexure-III	47
	Annexure-IV	51
	Annexure-V	52
	Annexure-VI	56

List of Tables

Table 1: Ocean Colour Monitor Sensor Specifications

Table 2: OCM-2 data coverage by Path and Row

Table 3: Level 2 flags considered to mask the land, ocean and clouds in generating the Level-2 Ocean Colour products

List of Figures

Figure 1: Spectral changes in OCEANSAT-II Ocean Colour Monitor (OCM)

Figure 2: OCM-2 data coverage across the Indian Ocean for LAC

Figure 3: SeaDAS main menu with OCM-2 module

Figure 4: Flow chart showing the data flow and generation of OCM-2 data products using SeaDAS software

Figure 5: Aerosol size distribution definitions

Figure 6: Typical change in aerosol size distribution definitions.

Figure 7: Relationship between the measured and estimated back scattering coefficient at

Figure 8: Relationship between chlorophyll concentration and absorption due to CDOM measured at 670nm

Figure 9: Flow chart showing generation of binned products from OCM-2

Figure 10: Geographical distribution of the sampling locations during the cruise period on 10th, 12th, 20th and 22nd of April 2011.

Figure 11: Comparison of chlorophyll-*a* concentration collected during the study period shows the vertical distribution for (a) Paradeep (b) Mahanadi and Haldia transects.

Figure 12: Spatial distribution of OCM-2 derived Chlorophyll-*a* concentration along the east coast of India on 10th, 12th, 20th and 22nd of April 2011 using SeaDAS software (OC2 algorithm).

- Figure 13:** Spatial distribution of OCM-2 derived Chlorophyll-*a* concentration along the east coast of India on 10th, 12th, 20th and 22nd of April 2011 using SeaDAS software (OC3 algorithm).
- Figure 14:** Spatial distribution of OCM-2 derived Chlorophyll-*a* concentration along the east coast of India on 10th, 12th, 20th and 22nd of April 2011 using SeaDAS software (OC4 algorithm).
- Figure 15:** Spatial distribution of OCM-2 derived Chlorophyll-*a* concentration along the east coast of India on 10th, 12th, 20th and 22nd of April 2011 using SeaDAS software (Chl-*a* algorithm).
- Figure 16:** Comparison of in-situ Vs satellite derived chlorophyll-*a* concentration using different bio-optical algorithms, for surface, middle and bottom depths of the sampling locations during the study period.
- Figure 17:** Geographical Spatial distribution and in-situ sampling site locations for Chl-concentrations in the Godavari basin during 02nd to 09th March 2012.
- Figure 18:** HPLC measured Chlorophyll-*a* concentrations compared with In-situ (radiometer) Chlorophyll-*a*
- Figure 19:** HPLC measured Chlorophyll-*a* concentrations compared with OCM-2 derived Chlorophyll-*a* concentrations.
- Figure 20:** Spatial distribution of Chlorophyll-*a* derived from OCM-2 on corresponding cruise dates

Summary

Satellite ocean-colour observations are now widely recognized as an important component of international remote sensing programs. Chlorophyll, the primary product of ocean-colour sensors, is a measure of marine phytoplankton biomass. Phytoplankton are responsible for approximately half the global photosynthetic uptake of carbon (Field *et al.*, 1998). In response to the potential importance of phytoplankton in the global carbon cycle and the lack of comprehensive data, the international community has established high priority satellite missions designed to acquire and produce high quality global ocean-colour data. In this regard the Indian Space Research Organisation took the leap in the field of Ocean Colour Remote Sensing by launching the first ocean colour sensor on board Oceansat-1 in 1992 with 8 spectral bands having a spectral resolution of 360m covering the entire North Indian Ocean. OCM-1 provided data for a period of ~10 years over the north Indian Ocean and then a continuation of this mission OCEANSAT-2 OCM was launched by ISRO on September 23, 2009 from Shriharikota by Polar Satellite Launch Vehicle (PSLV)-C14 rocket. The OCEANSAT-2 satellite carried three main instruments namely i) Ku band pencil beam Scatterometer, ii) Ocean Colour Monitor (OCM) and iii) Radio Occultation Sounder of Atmosphere (ROSA) instrument of Italian Space Agency (ASI). The OCEANSAT-2 OCM is mainly designed to provide continuity to the OCEANSAT-1 OCM instrument in 8 spectral bands but covering the entire global waters. The imaging principle of OCM is based on push-broom technique.

Ocean Color Monitor (OCM-2) instrument one of the payloads is designed to obtain quantitative information of ocean-colour variables e.g. chlorophyll-*a* concentration, vertical diffuse attenuation of the light, (K_d) and total suspended matter (TSM) concentration in coastal waters, apart from ocean-colour information OCM data will also be useful for studying the aerosol transport and terrestrial bio-sphere. Oceansat-2 Ocean Colour monitor being a global mission needs globally accepted geophysical data products. for this purpose we need to process OCM-2 data with uniform bio-optical algorithms, uniform atmospheric correction processed including flags, masks and other ancillary information which is globally accepted for the other Ocean Colour missions for generating the geophysical data products. Hence, we took an initiative to process OCM-2 data using the global ocean colour data processing software for generating the geophysical parameters. Apart from this the products generated by OCM-2 needs to be validated in both Indian as well as global waters for wide acceptance of OCM-2 products. Initially we validated OCM-2 data with three coastal cruises conducted in the Bay of Bengal in 2012. Further validation of the OCM-2 products in the global waters needs to be taken up.

1. Introduction

Satellite ocean-colour observations are now widely recognized as an important component of international remote sensing programs. Chlorophyll, the primary product of ocean-colour sensors, is a measure of marine phytoplankton biomass. Phytoplanktons are responsible for approximately half the global photosynthetic uptake of carbon (Field *et al.*, 1998). In response to the potential importance of phytoplankton in the global carbon cycle and the lack of comprehensive data, the international community has established high priority satellite missions designed to acquire and produce high quality global ocean-colour data. One of the goals of launching a number of ocean-colour sensors aboard various satellites is to build a long-term, multi-sensor, multi-year, ocean-colour archive (IOCCG, 1999; McClain, 1998). The derived chlorophyll concentrations (in time and space) can be used to resolve inter-annual-to-decadal changes in oceanic phytoplankton biomass in response to global environmental changes. Numerous obstacles stand in the way of this goal, including the different characteristics of the various sensors, (*e.g.* number of channels, their band widths and band centers, variations in the noise characteristics, differences in viewing geometry) as well as the differing approaches taken for the calibration of each sensor and the types of algorithms used to derive the appropriate geophysical quantities. Further, the methods used to average and quality control the basic pixel information, as well as the temporal and spatial binning schemes used to provide fields of geophysical quantities, also come into play when attempting to merge ocean-colour data from different sensors. The aim of the current working group / ocean colour team at National Remote Sensing Centre, ISRO is to examine issues related to the diversity in current “binning” schemes used for ocean-colour data, and to recommend one or more basic approaches that could be used across Agencies or projects, parallel to the current schemes. The goal of this report is thus to produce the best possible, large-scale representation of the current status of Ocean Colour data processing for generating the binned products accepted by the global community.

The aim of the report is not to define the best way to generate Level-3 ocean colour data products from Level-1 data of OCM-2 and generate binned products of OCM-2 as well as their application and validation of chlorophyll with the *in-situ* observations.

The following basic things have been addressed in this report

1. Introduction of the global processing software, SeaDAS
2. Generation of Level-2 geophysical data products from OCM-2 using SeaDAS for both LAC and GAC products
3. How to generate appropriate mean quantities for given variables to get the level-3 binned (gridded) products information relevant to both space and time scales
4. The atmospheric correction procedures implementation for better products generation using OCM-2
5. The importance of flags , thresholds and other ancillary information importance and their utility in generating the binned Ocean Colour products from OCM-2

2. Oceansat-2 Ocean Colour Monitor (OCM-2)

OCEANSAT-2 spacecraft of Indian Space Research Organization (ISRO) is the second satellite in ocean series, which was successfully launched on September 23, 2009 from Shriharikota by Polar Satellite Launch Vehicle (PSLV)-C14 rocket. The OCEANSAT-2 satellite carried three main instruments namely i) Ku band pencil beam Scatterometer, ii) Ocean Colour Monitor (OCM) and iii) Radio Occultation Sounder of Atmosphere (ROSA) instrument of Italian Space Agency (ASI). The OCEANSAT-2 OCM is mainly designed to provide continuity to the OCEANSAT-1 OCM instrument and OCM will collect data in 8 spectral bands and the imaging principle of OCM is based on push-broom technique. Ocean Color Monitor (OCM-2) instrument one of the payloads is designed to obtain quantitative information of ocean-colour variables e.g. chlorophyll-*a* concentration, vertical diffuse attenuation of the light, (*K_d*) and total suspended matter (TSM) concentration in coastal waters, apart from ocean-colour information OCM data will also be useful for studying the aerosol transport and terrestrial bio-sphere. OCEANSAT-2 OCM is almost identical to OCEANSAT-1 OCM, however central wavelength of two spectral bands i.e. band 6 and 7 have been shifted as shown in figure 1. The spectral band 6, which was located at 670 nm in OCEANSAT-1 OCM has now been shifted to 620 nm for improved

quantification of suspended sediments. The spectral band at 620 nm is also useful for substrate mapping of optically shallow coral reefs and other benthic ecosystems. The spectral band 7, which was located at 765 nm in OCEANSAT-1 OCM has been shifted to 740 nm to avoid oxygen (O₂A) absorption in OCEANSAT-2 OCM, this change is expected to improve the accuracy of the normalized water leaving radiance in shorter wavelengths obtained after doing the atmospheric correction. Table 1 provides the technical details of the OCEANSAT-2 OCM instrument.

Table 1: Ocean Colour Monitor Sensor Specifications

Parameters	Specifications
1. IGFOV at nominal altitude (m)	360 x 250
2. Swath (km)	1420
3. No. of spectral bands	8
4. Spectral range (nm)	402- 885
5. Spectral bands	B1 : 404-424 nm B2: 431-451 nm B3: 476-496 nm B4: 500-520 nm B5: 546-566 nm B6: 610-630 nm B7: 725-755 nm B8: 845-885 nm
6. Quantization Bits	12
7. Along track steering	± 200
8. Data acquisition modes	Local Area Coverage (LAC) - 360m X 236m Resolution Global Area Coverage (GAC)- 1 km x 1 km Resolution

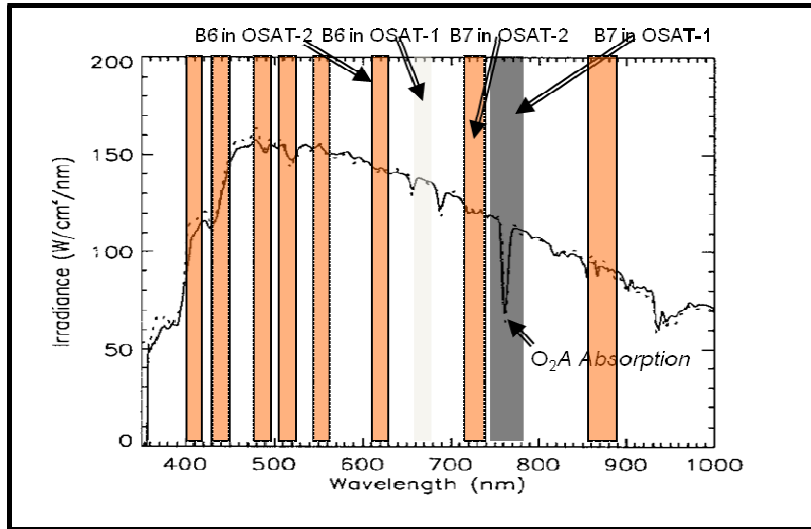


Figure 1: Spectral changes in OCEANSAT-II Ocean Colour Monitor (OCM)

3. Visibility / Coverage of OCM-2 Sensor for LAC data Products

The OCM-2 data passes with the respective path and rows covering the entire Indian Ocean have been procured and are listed in table 2. A set of 15 scenes covering the entire North Indian ocean (Bay of Bengal and Arabian sea) were used in this study. The data coverage of OCM-2 sensor with 5 degree elevation angle over the Indian Ocean is as shown in the figure 2.

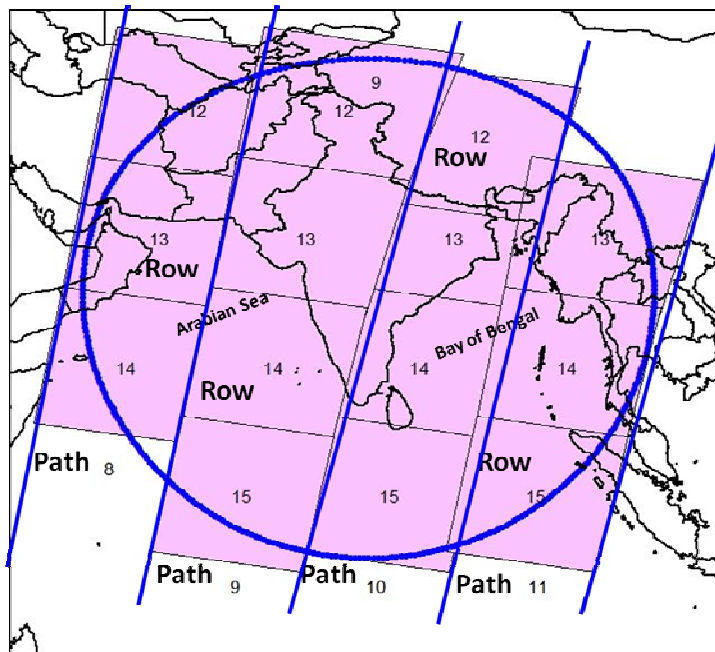


Figure 2: OCM-2 data coverage across the Indian Ocean for LAC

Table 2: OCM-2 data coverage by Path and Row

S.No	Path	Row
1	8	12
2	8	13
3	8	14
5	9	12
6	9	13
7	9	14
8	9	15
9	10	12
10	10	13
11	10	14
12	10	15
13	11	13
14	11	14
15	11	15

4. OCM-2 Data Products and their Representation

The standard products Local Area Coverage (LAC) of OCM-2 have the following condensational representation for as:

O2_05MAR2012_010_013_LAP_L1B_ST_S

O2_05MAR2012_010_013_GAP_L1B_ST_S

OceanSat-2 dd/mm/yy path_row LocalAreaProduct Level1B Standard
GlobalAreaProduct

Different levels of data products are available from OCM-2 for various applications as:

Level 0:

The Level 0 data of OCM-2 are unprocessed instrument/payload data at full resolution. Any artifacts of the communication (e.g. synchronization frames, communication headers) of these data from the spacecraft to the ground station have been removed. These data are the most raw format available, and are often not provided to end-users.

The L1A to L3 data files are in the HDF file format which store a variety of data types and meta data in a single file.

Level 1: The Level1 data of OCM-2 are available in two formats Level 1A and Level 1B.

Level 1A data are reconstructed, unprocessed instrument data at full resolution, time-referenced and annotated with ancillary information including radiometric and geometric calibration coefficients and georeferencing parameters (e.g. platform ephemeris data) computed and appended but NOT applied to the Level 0 data.

Level 1B data are Level 1A data that have had instrument/radiometric calibrations applied. The radiometrically corrected raw Oceansat-2 OCM data products are in the Hierarchal Data Format (HDF4.0).

Level 2: Level 2 data consist of derived geophysical variables at the same resolution as the source Level 1 data

Level 3: Level 3 data are the derived geophysical variables binned/mapped to a uniform space/time grid scale.

5. Processing of OCM-2 data using SeaDAS Software

OCM-2 being a global sensor provides high resolution chlorophyll products for global ocean colour applications. Hence, there is a need to generate the ocean colour products compatible with the other contemporary global ocean colour sensor's data in terms of processing platforms, atmospheric correction strategies, thresholds, flags and other stringent components like sun glint correction. In this context we adopted the global processing package namely, the SeaDAS: SeaWiFS Data Analysis System (SeaDAS), which is a comprehensive image analysis package for the processing, display, analysis and quality control of ocean color data developed and supported by NASA (<http://seadas.gsfc.nasa.gov>). SeaDAS version 6.2 software is intended to support the previous and current and upcoming ocean colour sensors like SeaWiFS, MODIS, OCTS, CZCS, MERIS and OCM-2 as well. The latest version of SeaDAS is able support the NPP/VIIRS data products also.

SeaDAS is globally accepted ocean colour data analysis software equipped with advanced processing features. Although it was originally used for SeaWiFS processing, recent upgrades have included the ability for SeaDAS to read in OCM-2 data, display L2 flags, and remap level 2 granules. It is an user-friendly software through open source with flexibility in processing by adjusting the parameters. It also has an objective in selection of alternative processing methods and used to reproduce all the standard ocean colour products of Levels 1, 2, and 3. This SeaDAS runs on Linux, Windows, Macintosh and also on Unix like systems. The software can be operated in different modes like Graphical user Interface (GUI), SeaDAS command line, UNIX command line and also using the IDL or Shell scripts. The SeaDAS is fully compatible with all the HDF-EOS data formats. The SeaDAS GUI and the data visualization /manipulation functions are written in the Interactive Data Language (IDL) which is a scientific programming language.

Though the Processing of OCM-2 has been incorporated in SeaDAS processing, the ICON in the main menu bar was not available for processing like the other ocean colour sensors data. We in collaboration with INCOIS and NIO, Goa took an initiative to generate an GUI based SeaDAS processing software for quick and easy processing of OCM-2 data like the other ocean colour

sensors. Prior to this OCM-2 used to be processed using 'command mode' only. The new GUI based OCM-2 processing main menu is shown in figure 3, has many advantages like we can select the parameters we need to get, we can change the processing options, select the atmospheric correction algorithms, aerosol models, time and spatial binning options and we can plug the meteorological / ancillary data for near real time processing and can give forecasts like PFZ etc with this now.

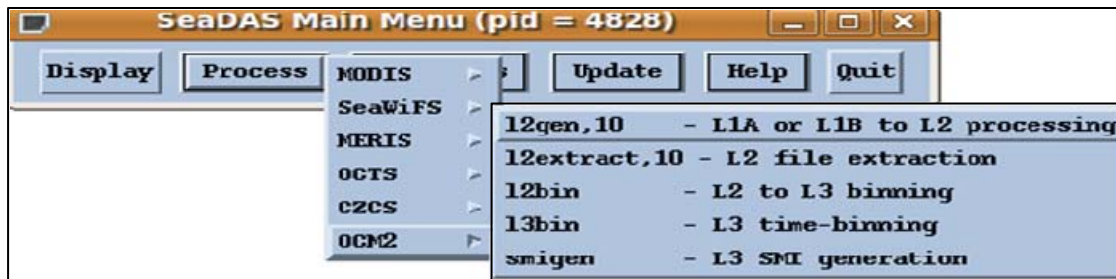


Figure 3: SeaDAS main menu with OCM-2 module

6. Methodology

The present processing sequence of OCM-2 in SeaDAS v.6.2 involves the conversion of level1b (L1B) data to level3 (L3) format. In the process of generating the L2 products which involve different processing methods along with atmospheric correction, flagging and masking with appropriate thresholds for cloud, land and glint affected areas / pixels a correction of suitable algorithm will be applied for the study locations for that scene/area, which were discussed in detail. It can generate nearly 53 Level 2 data products generation and new subroutines for new algorithms can also be upgraded in this package. The methodology and the processing sequence involved in OCM-2 processing using SeaDAS software is shown in figure 4.

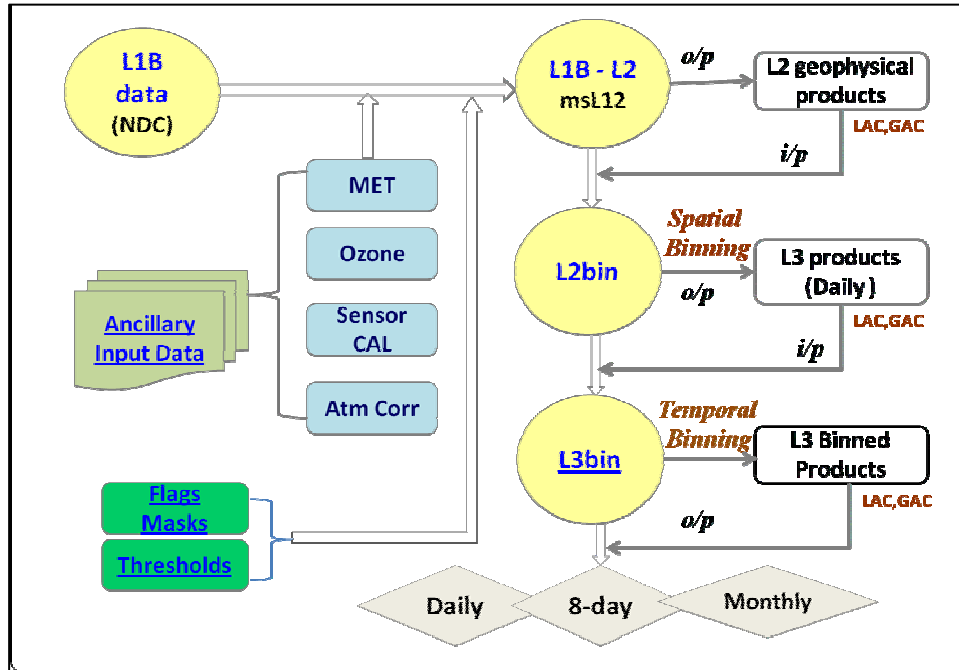


Figure 4: Flow chart showing the data flow and generation of OCM-2 data products using SeaDAS software

6.1 Atmospheric Correction

In oceanic remote sensing, the total signal received at the satellite altitude is dominated by radiance contribution through atmospheric scattering processes and only 8–10% of the signal corresponds to oceanic reflectance (Chauhan *et al.*, 2003). Before any interpretation and detection of the ocean colour data in the retrieval of ocean colour parameters from space such as chlorophyll concentration in near shore waters involves two major steps, the first is atmospheric correction of visible channels to obtain normalized water leaving radiance, $\rho_w(\lambda)$ and the second is the application of bio-optical algorithms for water parameters retrieval. Therefore, it becomes mandatory to correct for atmospheric effect, to retrieve any quantitative parameter from space. The goal of atmospheric correction applied to space acquired ocean colour observations is to retrieve the water-leaving radiances at the sea level from the total radiance recorded at the top of the atmosphere (TOA), Gordon and Wang (1994) developed the basic atmospheric correction algorithm based on single-scattering algorithm for non-absorbing aerosols. The atmospheric

correction algorithm employed by the NASA Ocean Biology Processing Group requires an assumption of negligible water-leaving reflectance in the near-infrared region of the spectrum. For waters where this assumption is not valid, an optical model is used to estimate near-infrared water-leaving reflectance.

6.2 Concept of NIR Correction

The total reflectance at a wavelength, λ measured at the top of the atmosphere as

$$\rho_t(\lambda) = \rho_r(\lambda) + \rho_a(\lambda) + \rho_{ra}(\lambda) + \rho_g(\lambda) + t\rho_w(\lambda) \dots\dots\dots(1)$$

TOA Rayleigh aerosol air glint water

where, ρ_r is the reflectance from multiple scattering by air molecules (Rayleigh scattering), ρ_a is the reflectance resulting from multiple scattering by aerosols, ρ_{ra} is the interaction term between molecular and aerosol scattering, ρ_g is the reflectance of the direct solar radiation, i.e., photons that are specularly reflected from the (rough) ocean surface, and ρ_w is the water leaving reflectance. In the CZCS atmospheric-correction algorithm the term ρ_{ra} is ignored, and it is assumed that ρ_a can be replaced by its single-scattering value ρ_{as} . Then the equation (1) becomes

$$\rho_t(\lambda) = \rho_r(\lambda) + \rho_{as}(\lambda) + t\rho_w(\lambda) \dots\dots\dots(2)$$

Where

$$\rho_{as}(\lambda) = \omega_a(\lambda)\tau_a(\lambda)p_a(\theta, \theta_o, \lambda)/4 \cos\theta \cos\theta_o$$

$$p_a(\theta, \theta_o, \lambda) = p_a(\theta_-, \lambda) + [r(\theta)+r(\theta_o)]p_a(\theta_+, \lambda)$$

$$\cos\theta_{\pm} = \pm \cos \theta_o \cos \theta - \sin\theta_o \sin\theta \cos(\dots\dots) \dots\dots\dots(3)$$

and $r(\theta)$ is the Fresnel reflectance for an incident angle θ . The parameters τ_a , ω_a , p_a are, the aerosol optical thickness, the aerosol single-scattering albedo, and the aerosol scattering phase function for a scattering angle. The angles θ_o and ϕ are the zenith and azimuth angles, respectively, of a vector from the point on the sea surface under examination (pixel) to the sun; likewise, θ and ϕ are the zenith and azimuth angles of a vector from the pixel to the sensor.

6.3 Aerosol Model selection for Atmospheric Correction

In SeaDAS processing of OCM-2 data, a set of aerosol models has been implemented for atmospheric correction based on the range of single-scattering albedos and aerosol size distributions retrieved from maritime AERONET sites. The size distributions were stratified by relative humidity (RH) and catalogued by fine and coarse-mode radii with fixed modal width as shown in figure 5. Eight RH-specific families of models were then constructed, each family spanning ten fine-to-coarse mode size fractions from 0.0 to 0.95.

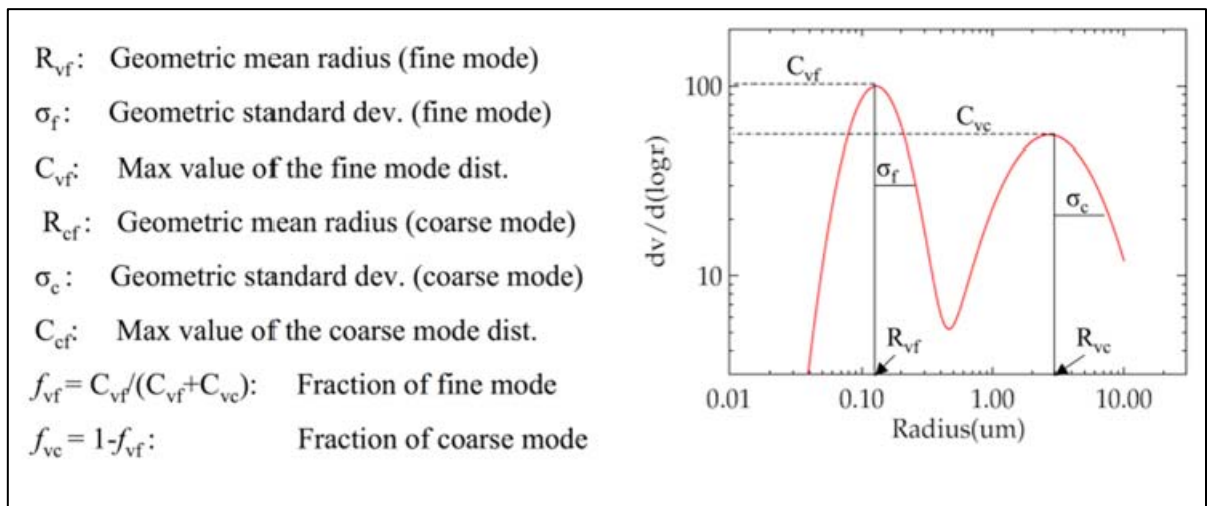


Figure 5: Aerosol size distribution definitions

The 80 aerosol size distributions and associated albedos were then processed through a vector radiative transfer code to produce the aerosol phase functions, single-scattering epsilons, single-to-multi-scattering relationships, and transmittance coefficients, as described in Gordon and Wang (1994), for the range of sensor wavelengths and observed viewing and solar radiant-path geometries (Ahmad et al.,2012). Nearly 80 look-up tables were then generated (one per size distribution) in an HDF format consistent with previous reprocessings. This simulation process was integrated into the distributed data processing system of the OBPB, thereby making it possible to produce a full set of tables for 80 models for each sensor.

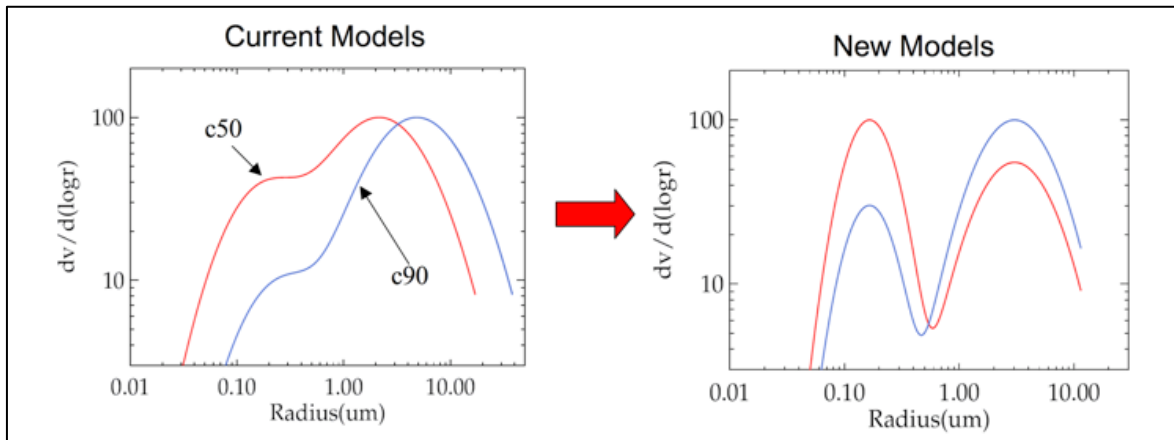


Figure 6: Typical change in aerosol size distribution definitions.

The aerosol model selection process was also modified to take advantage of the RH stratification and the RH information associated with each observation (from ancillary NCEP meteorological inputs/Climatology data). The ancillary RH information is used to select the two RH-specific families of aerosol models which bound the observation (figure 6). The model selection process is then executed independently on each family of 10 models, and the resulting aerosol reflectance retrievals are interpolated to the RH of the observation.

A critical component of this atmospheric correction algorithm is estimation of spectral aerosol reflectance, $\rho_a(\lambda)$, which are subtracted from the total measured signal as part of the process of determining $R_{rs}(\lambda)$. The algorithm implemented by the NASA Ocean Biology Processing Group (OBPG) requires an assumption of negligible water-leaving reflectance in the near infrared (NIR) region of the spectrum (i.e., $R_{rs}(\text{NIR}) = 0 \text{ sr}^{-1}$). The NIR bands for the OCM-2 Sensor (SeaWiFS) are centered on 745 and 866 nm. With this ‘black-pixel’ assumption, the measured top-of-atmosphere (TOA) reflectance in two NIR bands can be used to estimate both the magnitude and spectral dependence of $\rho_a(\text{NIR})$. Unfortunately, this assumption is rarely valid for waters with significant particulate (e.g., algal and mineral) backscattering (Siegal et al., 2000). If $R_{rs}(\text{NIR})$ can be modelled, however, it can be removed from the TOA signal, allowing the atmospheric correction to proceed in estimating $\rho_a(\text{NIR})$ as if $R_{rs}(\text{NIR})$ were negligible.

The OBPG implemented a bio-optical model to estimate $R_{rs}(\text{NIR})$ as part of the third reprocessing of the SeaWiFS mission in May 2000. This approach required an atmospheric correction process (ignoring $R_{rs}(\text{NIR}) > 0 \text{ sr}^{-1}$) to estimate the Chlorophyll-*a* concentration. This preliminary Chl-*a* was used to estimate spectral particulate backscattering, $b_{bp}(\text{NIR})$, which used to reconstruct $R_{rs}(\text{NIR})$. With this modeled $R_{rs}(\text{NIR})$ removed from the TOA signal, the process was repeated and Chl-*a* was recalculated, the process was iterated until convergence in Chl-*a* was achieved [Siegal et al., 2000 & Morel et al., 1998].

With the fourth SeaWiFS reprocessing in July 2002, this Chlorophyll driven algorithm was replaced with a reflectance based algorithm (Stumpf et al., 2003). The depression in the ratios of $\rho_a(\text{NIR})$ has been observed from the Siegal et al., (2000) in optically complex waters, this has been replaced by the model developed by Stumpf et al., (2003). This resulted in the selection of spectrally flat aerosol models within the atmospheric correction process, which artificially depressed the final Chlorophyll-*a* retrievals. In this revised model, $R_{rs}(\lambda)$ from an initial run through the atmospheric correction process and empirical estimates of the absorption coefficients for particles and dissolved materials at 670-nm were used to estimate $bbp(670)$ via an ocean surface reflectance model (Gordon et al., 1988). A spectral scattering function (Gould et al., 1999) was then used to derive $bbp(\text{NIR})$ from $bbp(670)$. Finally, $R_{rs}(\text{NIR})$ was reconstructed from $bbp(\text{NIR})$, the atmospheric correction process was repeated, and the process was iterated upon until convergence in $R_{rs}(\text{NIR})$ was achieved.

6.4 Bio-optical Model for NIR Iteration

Remote sensing reflectance is proportional to the IOPs, specifically the marine absorption and backscattering coefficients, through:

$$R_{rs}(\lambda) = G(\lambda) X(\lambda) \dots\dots\dots(4)$$

where

$$X(\lambda) = bb(\lambda)/a(\lambda) + bb(\lambda) \dots\dots\dots(5)$$

$G(\lambda)$ is a function of the illumination conditions, water constituents, and sea-state, $bb(\lambda)$ is the total backscattering coefficient [$bbw(\lambda) + bbp(\lambda)$], and $a(\lambda)$ is the total absorption coefficient

$[a_w(\lambda) + a_p(\lambda) + a_g(\lambda)]$. The additional subscripts w, p, and g indicate specific contributions by water, particles, and dissolved material, respectively.

A minor inconsistency was found with the NIR reflectance models implemented with the fourth re processing of SeaWiFS data. For the R_{rs} (NIR) model look up tables (LUTs) were implemented (More *et al.*, 2002), for both the conversion of retrieved R_{rs} (VIS) to IOPs and the conversion of modeled IOPs to R_{rs} (NIR). While these LUTs were originally generated for waters whose light field is predominantly influenced by phytoplankton, which are proved suitable for use in this model.

6.5. Spectral Dependency of the IOP's

6.5.1. Backscattering

With the known absorption and the measured R_{rs} the back scattering coefficient can be obtained at a reference wave length i.e., 670nm, this estimated $b_b(\lambda_0)$ can be extrapolated to NIR wavelengths through a spectral model. The spectral dependency of the back scattering is expressed as

$$b_b(\lambda) = b_b(\lambda_0) \cdot Y \dots(6)$$

$$b_b(\lambda_0) = [b_{bw}(\lambda) + b_{bp}(\lambda_0)] \cdot Y \dots(7)$$

Where Y is parameterized as a power law function

$$Y = [\lambda_0 / \lambda]^\eta$$

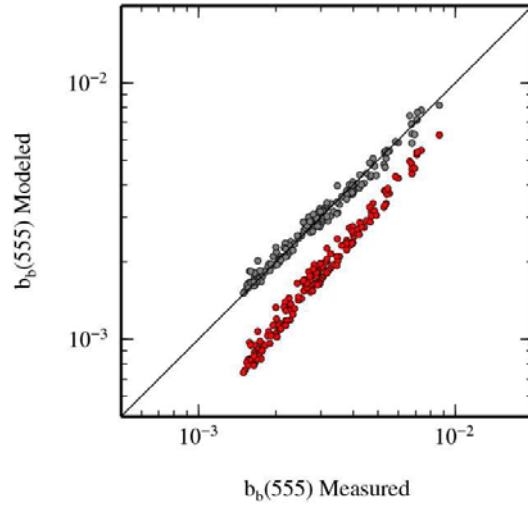


Figure 7: Relationship between the measured and estimated back scattering coefficient

According to Lee et al., (2010), the η term is typically in the range of [0, 2], with values around 2 observed in open ocean waters and turbid waters approaching zero. In the Rrs(NIR) model employed in R2009, the common power-law form of Eq. (7) was adopted. Rather than relying on a fixed η value, however, the empirical relationship developed Lee et. al., (2010) was adopted:

$$\eta = 2[1 - 1.2 * e^{(-0.9 * Rrs(443) / Rrs(555))}] \quad \dots\dots(8)$$

6.5.2 Absorption

In the NIR, the total absorption is dominated by the absorption due to water, $a_w(\lambda)$ (Pope & fry et al.,1997) such that absorption coefficients for particles and dissolved material at NIR radiances can be ignored. There were two functions one is based on chlorophyll concentrations (Bricaud et al., 2012) and the other is based on (figure 8) on the green to red reflectance ratio (Stumpf et al 2003), involved in this for the estimation of the total absorption coefficient, $a(670)$ for the inversion of Rrs to retrieve $bbp(670)$ where $a_p(670)$ and $a_g(670)$ can be a significant portion of the total.

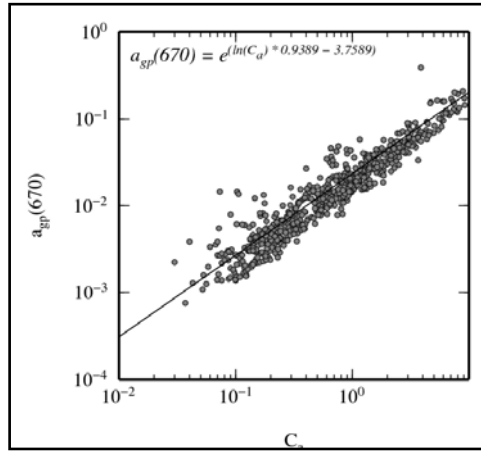


Figure 8: Relationship between chlorophyll concentration and absorption due to CDOM measured at 670nm

In the modified $R_{rs}(\text{NIR})$ model, this was updated to a single, chlorophyll based relationship derived from NOMAD (Type II linear regression using spectroscopy only, limited to Chl- $a > 0.2 \text{ mg m}^3$).

$$a(670) = e^{(\ln(\text{Ca}) * 0.9389 - 3.7589)} + a_w(670) \quad \text{----(9)}$$

The $a_p(670)$ and $a_g(670)$ values contained within the NOMAD data set span a range of $0.00001\text{--}0.03 \text{ m}^{-1}$ for $a_p(670)$ and $0.00057\text{--}0.8413 \text{ m}^{-1}$ for $a_g(670)$.

6.6. Iteration Method

The retrieval of $R_{rs}(\lambda)$ in highly scattering waters requires the estimation of $R_{rs}(\text{NIR})$, and further requires knowledge of $R_{rs}(\text{VIS})$, the $R_{rs}(\text{NIR})$ algorithm must be implemented iteratively. The iteration begins by assuming $R_{rs}(\text{NIR}) = 0 \text{ sr}^{-1}$, so that initial $R_{rs}(\lambda)$ can be derived and a first estimate of $R_{rs}(\text{NIR})$ can be achieved. The iteration converges when $R_{rs}(\lambda)$ changes by less than

2%. In the majority of cases, the method converges after 3-4 iterations, but the algorithm allows up to 10 iterations. If, however, the initial atmospheric correction results in negative or an otherwise nonphysical spectral distribution for $R_{rs}(\lambda)$ (criteria based on in situ observations), the iteration is re-initialized assuming $\rho_a(\text{NIR}) = 0$ (i.e., all reflectance except that from Rayleigh scattering and Sun glint originates from the water mass). This is effectively the opposite extreme from the initial condition of $R_{rs}(\text{NIR}) = 0 \text{ sr}^{-1}$. The iteration process is then allowed to proceed to convergence as previously described.

For the rare cases where the iteration fails to converge after this reset, an additional iteration is forced, again with an assumption of $\rho_a(\text{NIR}) = 0$. This pixel is then flagged with an ‘atmospheric correction warning’ to alert users to the questionable nature of the pixel, although a qualitatively useful retrieval may still result.

The controls on this iteration scheme differ slightly from previous implementations [8], especially with regards to the how the iteration is reset, which is currently more robust than that of past methods. It should also be noted that the $R_{rs}(\text{NIR})$ is forced to zero if the initial iteration results in a $\text{Chl-a} < 0.3 \text{ mg m}^{-3}$. Furthermore, to avoid the introduction of transitional artifacts, the $R_{rs}(\text{NIR})$ estimation is linearly weighted from 0 to 1 for $0.3 > \text{Chl-a} > 0.7 \text{ mg m}^{-3}$. The iteration is reinitialized on any iteration where the chlorophyll retrieval fails, up to the maximum allowed iterations (currently 10).

6.7. Ancillary Data information

The Ocean Biology Processing Group makes use of several sources of ancillary data in the level-2 data processing like Meteorological Data and the Climatological data.

The met parameters used in the L1 to L2 processing are

- Meridional and Zonal Wind - Water roughness predictions used for glint estimations.
- Pressure - Computes the atmospheric depth for Rayleigh radiance removal from total radiances.
- Humidity - Used to select the proper aerosol correction table.

- Ozone data of Ozone concentrations - Used to remove the effects of ozone absorption from the total radiances and the data source is EPTOMS , OMI, TOAST (combination of TOVS & SBUV *in-situ* data)

The data sources for these meteorological datasets are available from National weather Service's NCEP data. If the above files are not provided a climatology file is used as default.

6.8. Flags, Masks and Thresholds

6.8.1 FLAGS

As data is processed by msl12 from Level-1 to Level-2, checks are made for different predefined conditions. When certain tests and conditions are met for a given pixel, a **flag** is set for that pixel for that condition, and **the pixel is still processed**. A total of 32 flags can be set for each pixel. These msl12 "Level-2 processing flags" are stored in the Level-2 data file as the **l2_flags** product. The storage method sets bits to 0 or 1 in 32-bit integers that correspond to each flag.

6.8.2. MASKS

During data processing, the flags described above can also be used to determine which pixels are **not to be processed at all**. These predetermined conditions are called **masks**. For Level-1 to Level-2 processing (msl12), masked pixels are **not processed** and are typically set to zero so as to eliminate them from future analysis. (For products where zero could be a valid data value, a number outside the possible data range is substituted.) For SeaWiFS and MODIS, msl12 currently has 8 predefined L1A processing masks available (each defined by only one of the Level-2 flags). These can be turned on (1) or off (0) by the user. In the case of Level-2 to Level-3 processing (l2bin), any one or combination of the 32 standard Level-2 flags can be combined to construct the one available l2bin mask. Then during the processing if **all** the pixels in a given bin have been flagged as masked pixels, that bin will not be included in the Level-3 data file. These 8 masks and their default settings are listed in table 3.

Table 3: Level 2 flags considered to mask the land, ocean and clouds in generating the Level-2 Ocean Colour products

maskland	Mask out all land pixels: 0=off, 1=on. (Default=1).
maskbath	Mask out shallow water: 0=off, 1=on. (Default=0).
maskcloud	Mask out pixels for which cloud albedo is above user defined threshold: 0=off, 1=on. (Default=1).
maskglint	Mask out pixels with sun glint: 0=off, 1=on. (Default=0).
masksunzen	Mask out pixels with large solar zenith angle: 0=off, 1=on. (Default=0).
masksatzen	Mask out pixels with large sensor zenith angle: 0=off, 1=on. (Default=0).
maskhilt	Mask out pixels where total radiance greater than knee value: 0=off, 1=on. (Default=1).
maskstlight	Mask out pixels with stray light: 0=off, 1=on

6.9 Binning

Binning is the process of projecting and aggregating data from an arbitrary spatial and temporal scale into a uniform scale over a defined time range. The binning process preserves both the central tendency (e.g., average) and the variation in the data points that contribute to a bin. Level-3 spatial binning is performed on level-2 files and each L2 file is spatially binned to an equal-area grid. L3 files are the statistical data products that allow to calculate mean, standard deviation, median and mode for each L2 variable. Level-3 binned data product consists of the accumulated data for all the level-2 products for the sensor and the resolution and corresponding to the period of one day, 8-days, a calendar month or calendar year. The data are stored in the representation of

global equal area grids with standard bin sizes .The theoretical basis and the algorithms of binning process are reported in SeaWiFS PL Vol32.

The binned files are geophysical products averaged spatially and/or temporally and are limited to fixed binned resolutions of 500m, 1Km, 2Km, 4Km, 9km or 36km. A pixel from the parent level-2 product is excluded from binning if a bit in the parent level-2 products l2_flags corresponding to the pixel is set (equals1) and the algorithm name for that bit has been used for the exclusion by an input parameter to the binner. Generation of weekly, monthly and other desired binned products process is shown in figure 9.

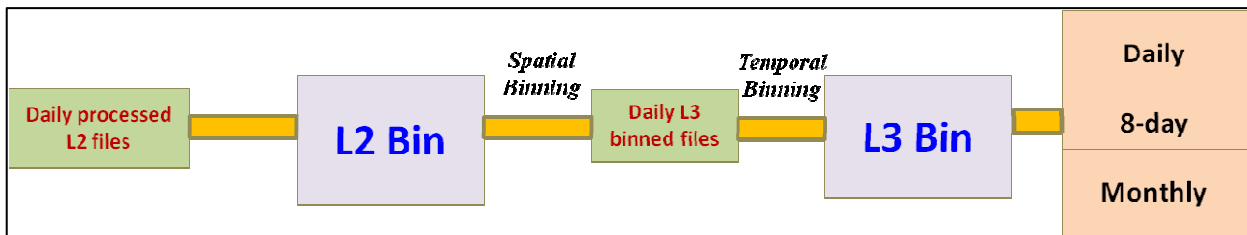


Figure 9: Flow chart showing generation of binned products from OCM-2

7. Validation of OCM-2 chlorophyll with *in-situ* measurements

7.1 Validation in the Coastal Waters of Off Mahanadi and Paradip

As a part of validation a coastal cruise was conducted in the coastal waters of Off Mahanadai, Paradip and Haladia regions at surface (0m), middle (5m) and deep (10-15m) on 10th, 12th 20th and 22nd April 2011. during The study area covers Ocean Colour Monitor (OCM-2) data of row:10 and path:13 covering Paradip (20⁰N, 86⁰E) Mahanadi (20.15⁰N, 86.12⁰E) and Haladia (21.6⁰N, 88.02⁰E) regions with 360m resolution has been utilised for this present study. The geographical distribution of the sampling locations was shown in figure (10).

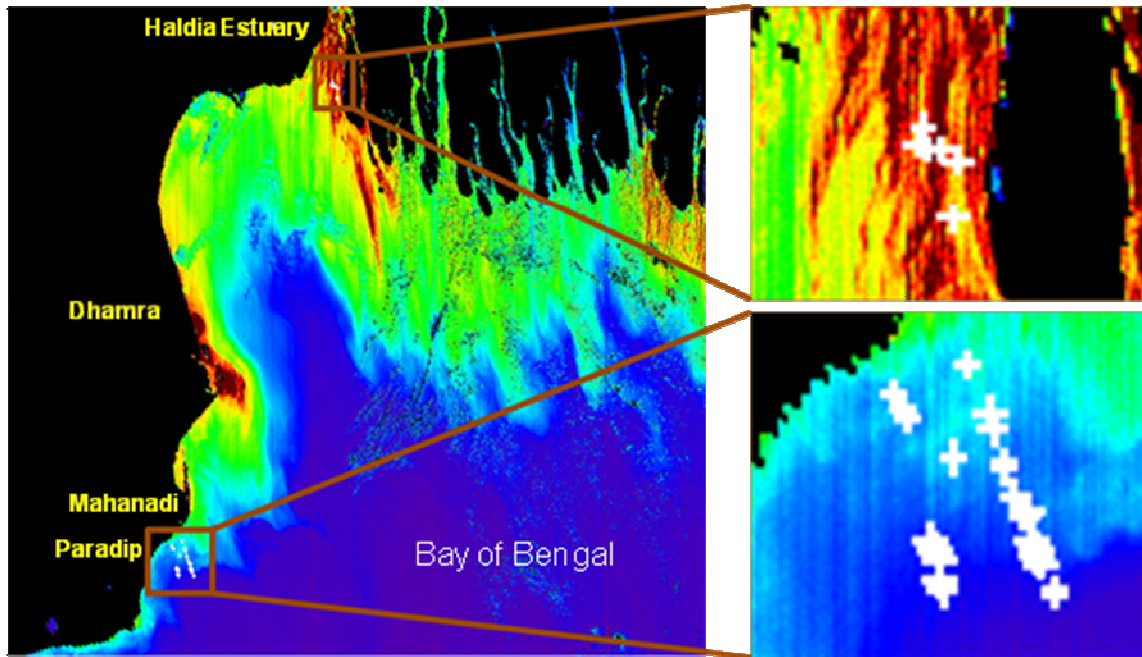


Figure 10: Geographical distribution of the sampling locations during the cruise period on 10th, 12th, 20th and 22nd of April 2011.

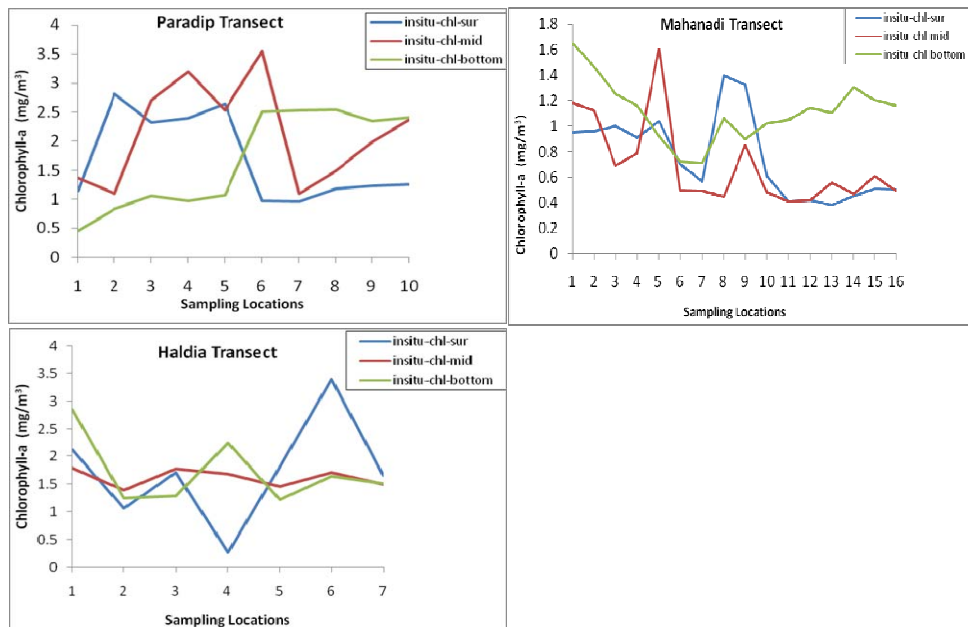


Figure 11: Comparison of chlorophyll-a concentration collected during the study period shows the vertical distribution for (a) Paradeep (b) Mahanadi and Haldia transects.

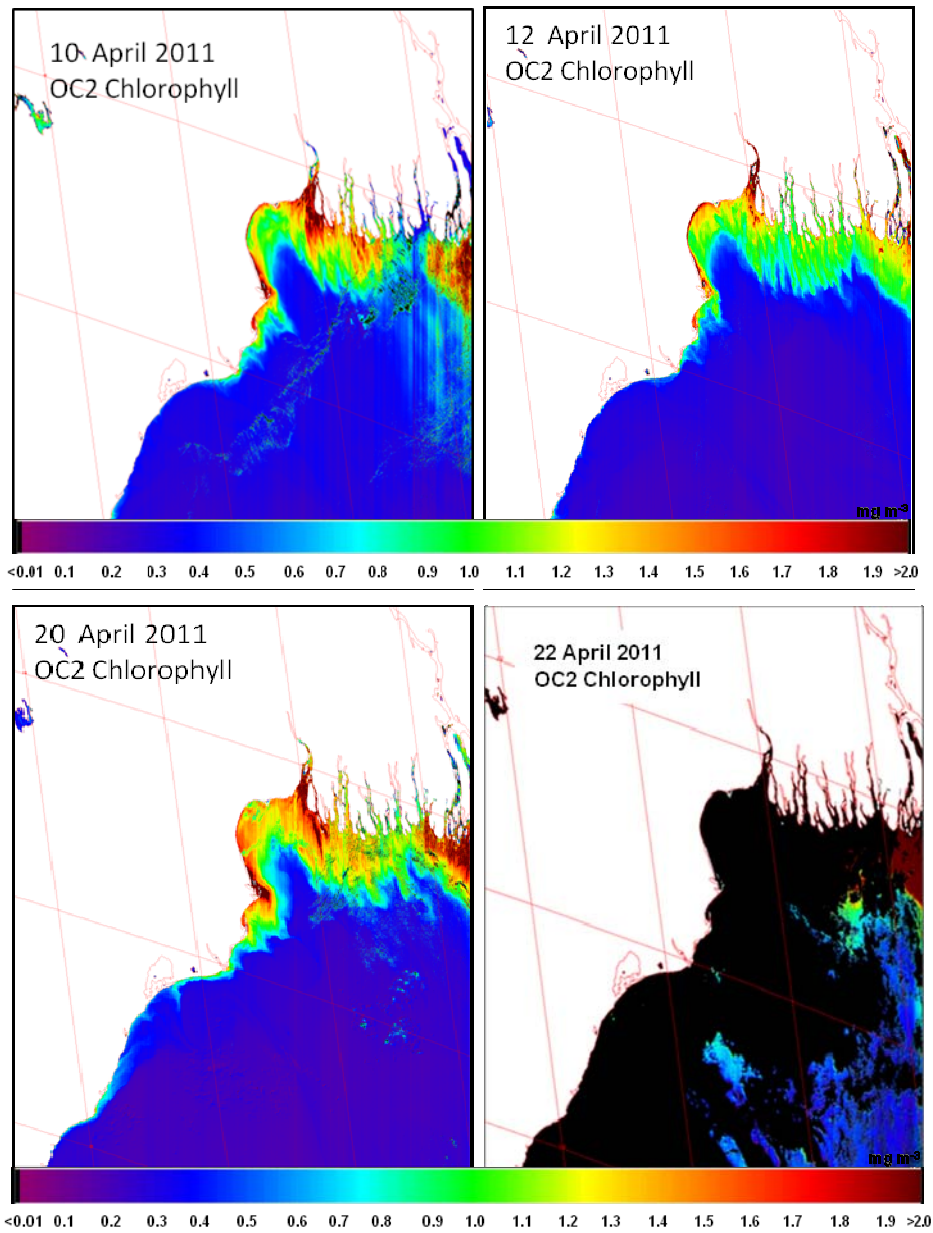


Figure 12: Spatial distribution of OCM-2 derived Chlorophyll-*a* concentration along the east coast of India on 10th, 12th, 20th and 22nd of April 2011 using SeaDAS software (OC2 algorithm).

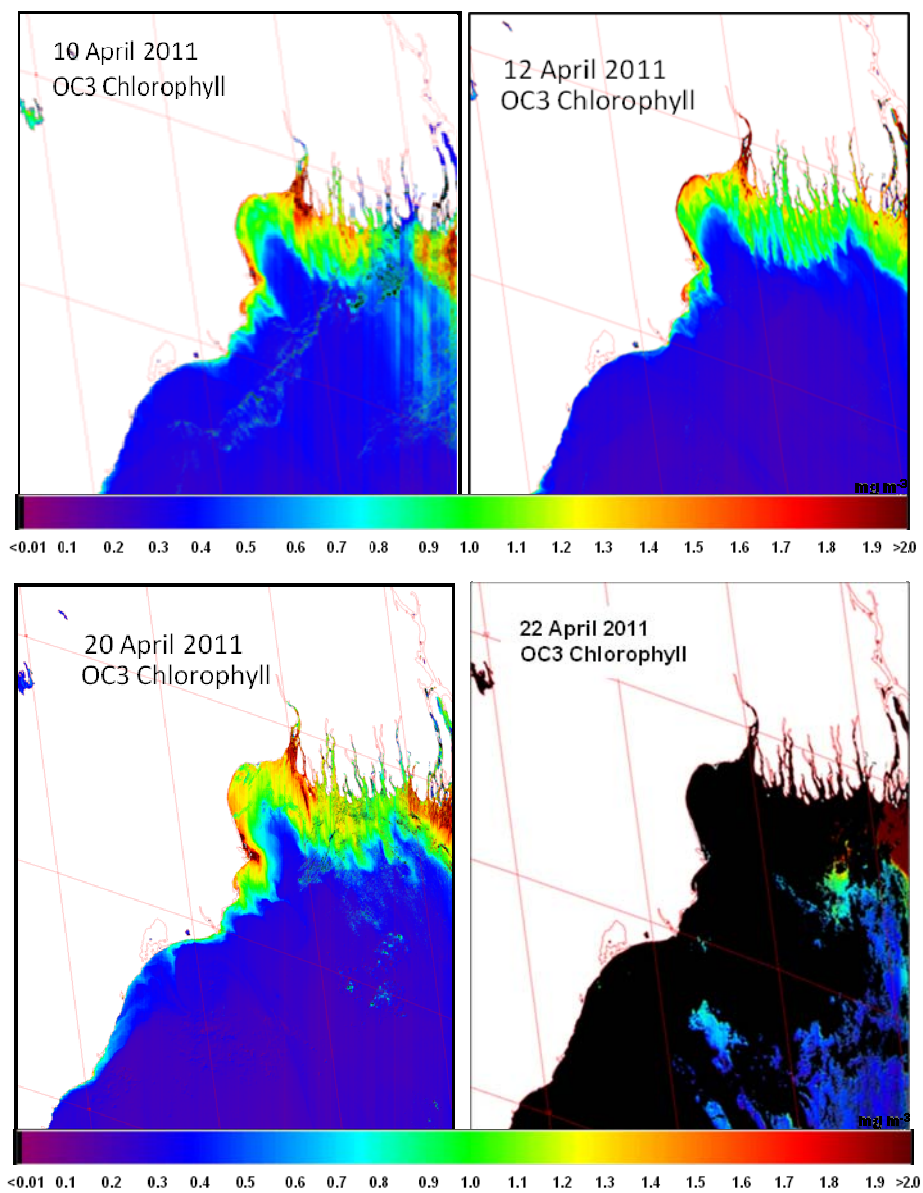


Figure 13: Spatial distribution of OCM-2 derived Chlorophyll-*a* concentration along the east coast of India on 10th, 12th, 20th and 22nd of April 2011 using SeaDAS software (OC3 algorithm).

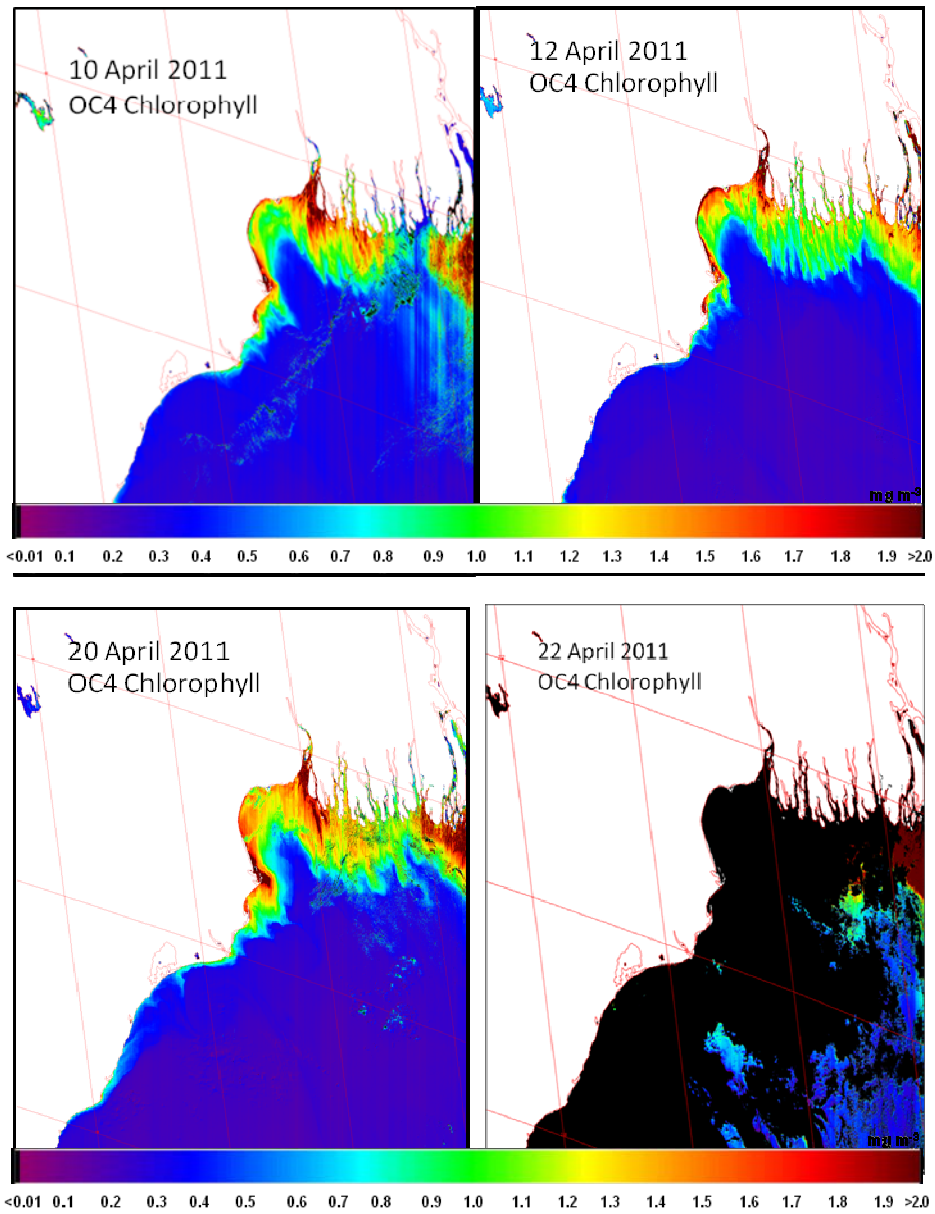


Figure 14: Spatial distribution of OCM-2 derived Chlorophyll-*a* concentration along the east coast of India on 10th, 12th, 20th and 22nd of April 2011 using SeaDAS software (OC4 algorithm).

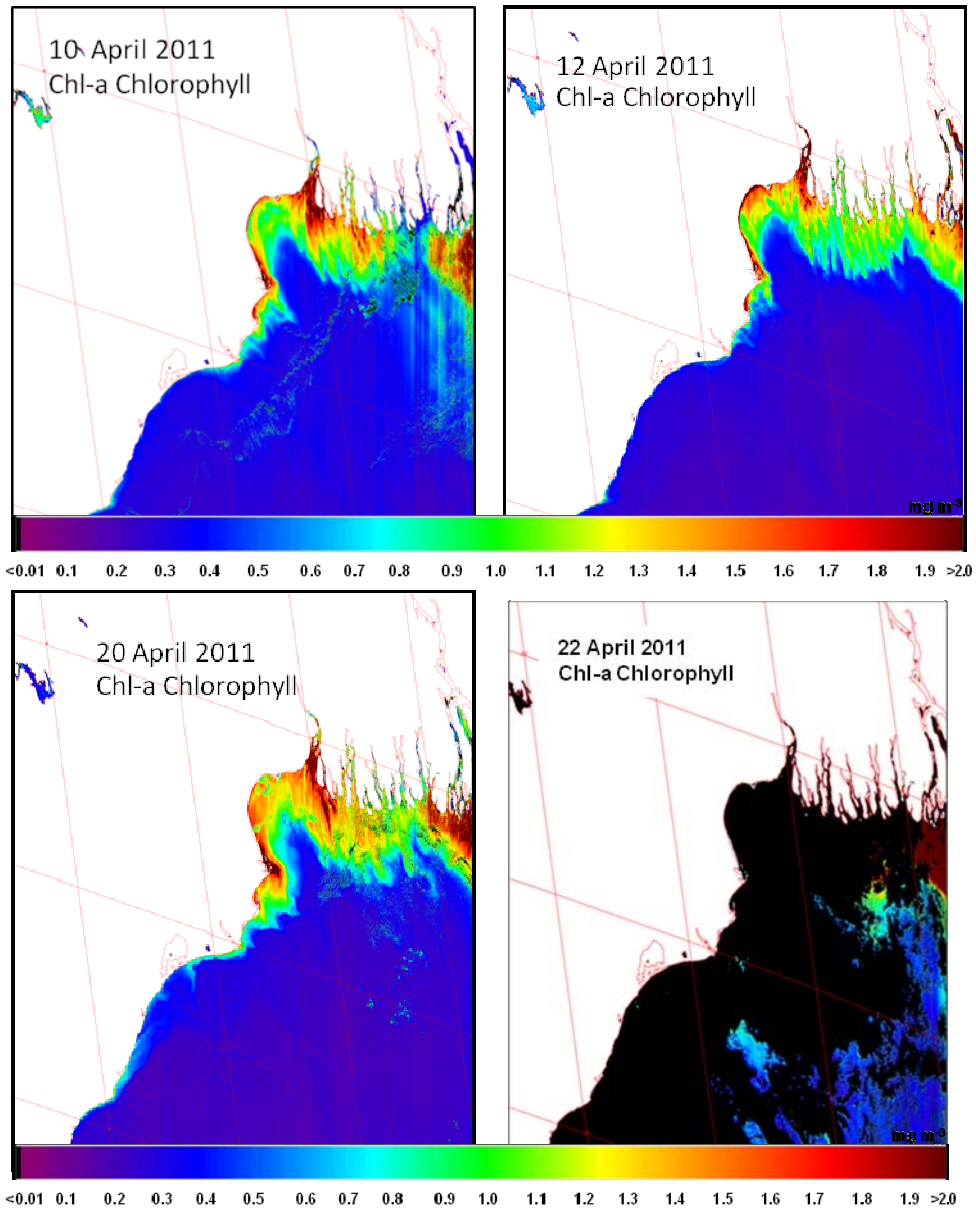


Figure 15: Spatial distribution of OCM-2 derived Chlorophyll-*a* concentration along the east coast of India on 10th, 12th, 20th and 22nd of April 2011 using SeaDAS software (Chl-*a* algorithm).

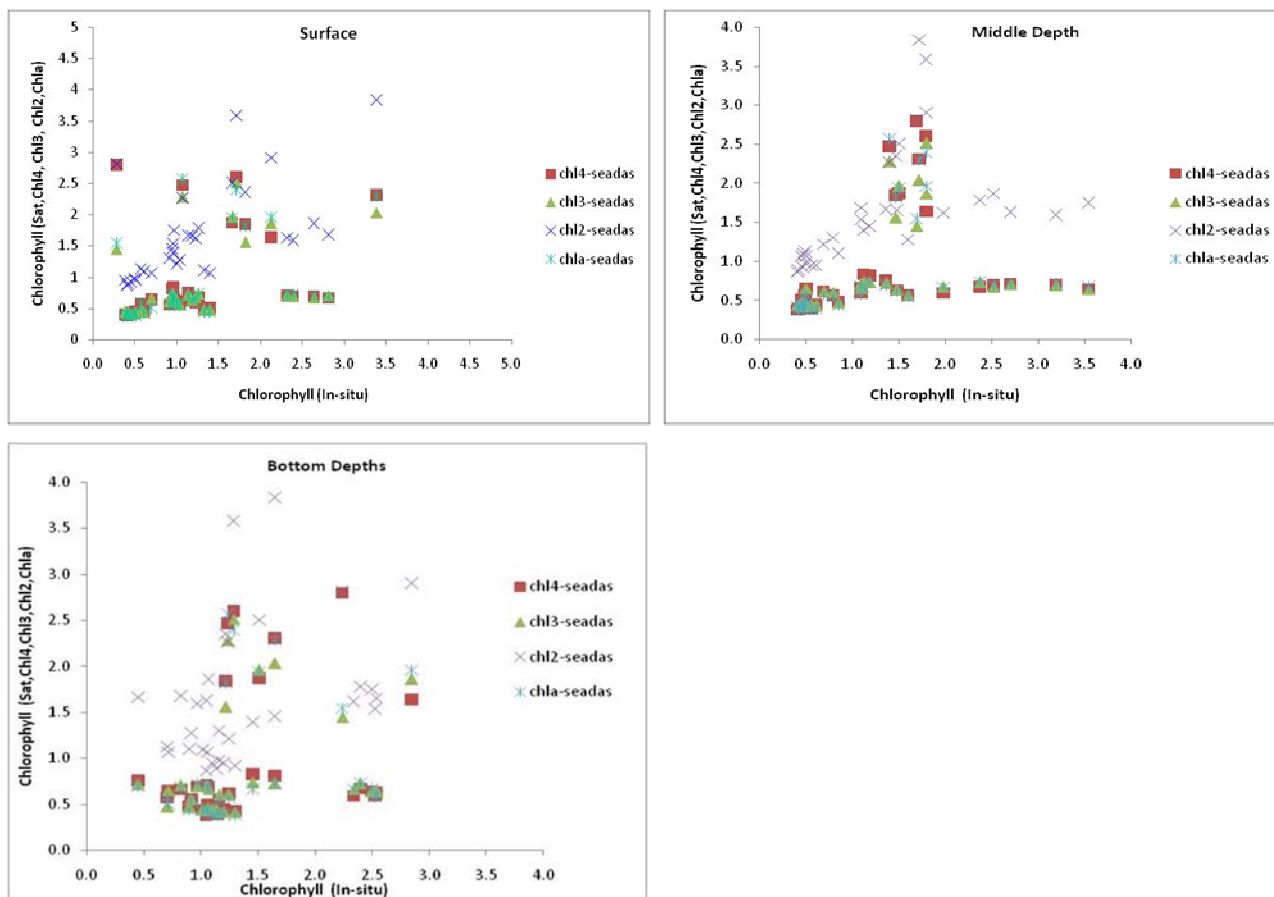


Figure 16: Comparison of *in-situ* Vs satellite derived chlorophyll-*a* concentration using different bio-optical algorithms, for surface, middle and bottom depths of the sampling locations during the study period.

As an initial analysis of the data distribution and chlorophyll-*a* variability the data collected for all the dates were plotted along the transect, as shown in figure 10. In this figure except the last date data i.e., the data collected on 22nd April 2011 was not plotted as that data set was discarded due to the presence of thick clouds over that region. From figure 16 the spatial distribution of chlorophyll-*a* along that transect, shows decrease in the chlorophyll-*a* concentration while moving away from the coast towards offshore waters (figure 16).

Chlorophyll-*a* concentration vary from a minimum value of 0.96 to a maximum value of 2.81 mg m⁻³ with a mean value of 1.69 mg m⁻³ at the surface; 1.09, 3.54 and 2.132 mg m⁻³ at the middle depth and 0.45, 2.54 and 1.67 mg m⁻³ at bottom depth as minimum, maximum and mean values respectively in Paradeep area. Chlorophyll-*a* concentration vary from a minimum value of 0.38

to a maximum value of 1.4 mg m^{-3} with a mean value of 0.76 mg m^{-3} at the surface; 0.41, 1.6 and 0.69 mg m^{-3} at the middle depth and 0.71, 1.65 and 1.11 mg m^{-3} at bottom depth as minimum, maximum and mean values respectively in Mahanadi region. Chlorophyll-*a* concentration vary from a minimum value of 0.28 to a maximum value of 3.39 mg m^{-3} with a mean value of 1.72 mg m^{-3} at the surface; 1.4, 1.8 and 1.62 mg m^{-3} at the middle depth and 1.22, 2.85 and 1.71 mg m^{-3} at bottom depth as minimum, maximum and mean values respectively in Haldia region (figure 11).

As mentioned in the methodology SeaDAS processing software was used to process the chlorophyll-*a* concentration using OC2, OC3, OC4 and Chl-*a* algorithms from OCM-2 data. The new gain coefficients modified on June 2010 provided by National Data Centre (NDC) along with the L1B data product (the gain coefficients were given in the header file of each scene of OCM-2) were used for converting the digital numbers into radiance values. The cloud masking value was set to 0.07 for OCM-2 based on the reflectance values of band 8 i.e., 865nm (according to the existing and proposed cloud masking algorithms of SeaWiFS and MODIS sensors). However, this threshold was set to 0.07 based on our internal studies for OCM-2 that was carried out to set the cloud masking threshold for processing OCM-2.

The chlorophyll-*a* images generated using OC2, OC3, OC4 and Chl-*a* algorithms for the study period are shown in figure 12, figure 13, figure 14 and figure 15 respectively. In all these figures the chlorophyll-*a* image generated on 22nd April 2011 shows most of the region that was masked, represented with black colour. The land portion that was masked is shown in white colour for demarcating from cloud and land pixels. The valid ocean pixels were only considered for interpreting the data during the study period and the chlorophyll-*a* variability of those pixels are represented in colour for better understanding of chlorophyll-*a* distribution in the open as well as coastal ocean regions. From these figures it is clearly understood that the chlorophyll-*a* variability in the open ocean region vary from 0.05 to 0.1 mg m^{-3} only and the concentration increases towards the coast.

As a part of validation the *in-situ* measured chlorophyll-*a* concentration has been compared with satellite derived chlorophyll-*a* (figure 16) during the study period processed using various

chlorophyll-*a* algorithms. These results were plotted as a scatter plot for better understanding the algorithms performance in the coastal waters using OCM-2 data, which was shown in figure 7. From this figure it has been shown that the existing global ocean colour algorithms over estimates in the near shore coastal waters as well as estuarine region - Haladia. Where not only the chlorophyll concentration plays a major role like the sediment re-suspension, pigment and the shell structure which is being formed by calcification. The costal system is more optically complex because of short-term coastal upwelling, enhancement of nutrients because of river run-off and anthropogenic activity and biological process like nitrification, de-nitrification, carbonate system etc which has direct bearing with phytoplankton growth and their pigment characterization. Besides the area is dominated by unicellular diatoms basically contains silica. Hence the costal process becomes more complex in terms of bio-geo chemical behavior. Hence retrieval of chlorophyll becomes erroneous in its quantification. This requires specific, suitable regional bio-optical algorithms to overcome this problem.

A rigorous statistical analysis was carried out for the *in-situ* estimated and the chlorophyll-*a* concentration estimated using the global ocean colour algorithms. For this purpose the values like standard deviation (SD), root mean square error (RMSE), %error, slope intercept, the regression coefficient (R), bias and the scatter index (SI) were calculated for all the data points collected used for validation. For this purpose the data was segregated into three sets for surface, middle and bottom depths by combining all the stations data from Paradeep, Mahanadi and Haldia regions.

Although the OC4 and OC3 algorithms over estimate in the coastal waters OC2 performs better in the lower concentration range near Paradip, Mahanadi and Hugli estuary near Haldia. The total distribution of chlorophyll-*a* concentration in the Hugli estuary some times over estimated due to the presence of overlap or dominance of chlorophyll-*b* pigments will lead to mislead the estimation of chlorophyll-*a* concentration in this region.

7.2 Validation in the Coastal Waters of Godavari Basin

As a part of validation of Oceansat- OCM data products for Ocean Colour application another coastal cruise was conducted in the coastal waters of Godavari basin from 2-9th March 2012. The geographical distribution and the sampling locations of the study area are shown in figure 17.

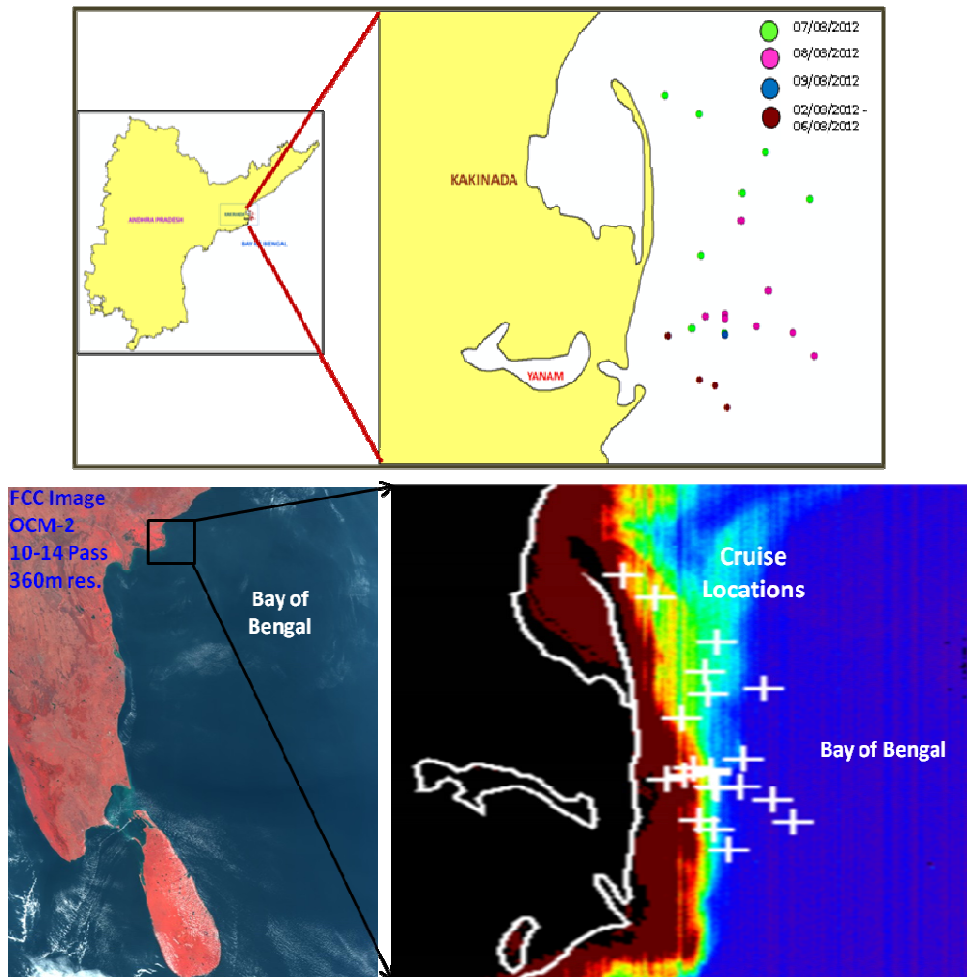


Figure 17: Geographical Spatial distribution and *in-situ* sampling site locations for Chl-a concentrations in the Godavari basin during 02nd to 09th March 2012.

7.2.1 *In-situ* data processing

The raw radiometric profiles collected using Hyperpro-II were processed using Prosoft 7.7.16 software to extract the radiance parameters collected onboard the vessel by loading all

instrument configuration information i.e., the calibration files of the sensors embedded in the instrument and loading the processing parameters by applying dark correction to the data when averaging. In this processing chain we used the multilevel processing i.e., from L1a raw binary data to L4 generated data product and processing was carried out by applying the calibration data to all optical and ancillary sensors for conversion of binary data, by corrections and checks which include pressure tare correction, wavelength sequence, tilt angle for quality control and finally to generate the data product of radiances. In the extraction of chlorophyll concentration profiles of Fluorometer at each depth Morel (2001) model has been used and the SeaBAM and Gordon models for the estimation of surface water chlorophyll concentrations. In order to validate the *in-situ* data with the satellite data the fluorometric measurements of chlorophyll-*a* concentrations were averaged to a subsurface depth of 5m.

7.2.2 Study Area

Godavari is the largest of Indian peninsular rivers; the river divides into two main distributaries Gautami and Vasishta which gives rise to a sprawling estuarine deltaic system fringed with tidal creeks and dense mangrove forests before reaching the Bay of Bengal. The Godavari estuary is well mixed up with the tidal effect dominating in the lean season. The area between the Gautami-Godavari and Kakinada bay has dense vegetation of mangrove forests and mudflats. The shallow Kakinada bay opens into the sea on its northern side and is bordered along by a narrow sand bar. The coastal morphology of this entire Godavari regime has been explained in detailed by K.N. Rao et al., (2003). The continental shelf of the region is relatively narrow which is located 20km north of the Godavari delta. The 10m to 30m depth contours in this region are 10km away from the shore and 50, 75, 100m depth contours are ranging from 20 to 30km from the shore.

The study area encompasses the coastal waters of the Godavari basin along Off Kakinada and Yanam during March 1-10, 2012 covering 21 stations from $16^{\circ} 41.125'N$ to $16^{\circ} 58.099'N$ latitudes and $82^{\circ} 32.141'E$ to $82^{\circ} 23.425'E$ longitudes. Figure 17 shows the geographical distribution of the locations of *in-situ* data collected. Among all the 21 stations, 19 stations covers the Coastal waters (Case-2) at varying depths from surface to 75m whereas 2 stations

covers the intermediate waters (almost offshore waters) varying from 100m to 150m of depth covering the Kakinada Bay and Gautami Godavari estuarine region of the Bay of Bengal. The first four stations as shown in figure(1) were covered in all the days from 02 to 05 of March 2012 and the other 17 stations are covered during 06 to 09 of arch 2012.

7.3 Materials and Methods / Data Collection

7.3.1 Instruments Used - Hyperpro-II

Hyperspectral Underwater radiometer (Hyperpro-II; Satlantic Inc.) measures the colour of the ocean and its spectral variability throughout the euphotic zone. It provides observations of the optical properties of the ocean to investigate the fundamental biological and physical processes that involve light in the ocean. The optional integration of the foreign sensors (Wet Labs ECO Series) within Hyperpro-II is used for determination of other parameters like chlorophyll fluorescence, CDOM absorption, Backscattering etc. The chlorophyll fluorescence serves as a valuable indicator of active phytoplankton biomass and chlorophyll concentration in waters. These measurements are used for tracking biological variability and abundance in the water column. The present modular design of the Profiler II allows the system can be configured by Satlantic to be either a free-falling profiler or with detachable float for near-surface measurements and minimizes the size and weight of the profiler, allowing rapid deployment from even small boats where Irradiance and Radiance measurements can be collected as close as 5cm from the sea surface.

The instrument was calibrated to a wavelength range of 350-800nm used to measure the underwater radiation fields in profiling mode using the Satlantic HyperOCR series of digital optical sensors with a 10 degree $\frac{1}{2}$ angle field of view in water(R10W) depending on the instrument availability which are connected to the instrument body to measure upwelling radiance, $L_u(z)$, upwelling irradiance, $E_u(z)$ and downwelling irradiance, $E_d(z)$ with a reference sensor for the surface irradiance measurements, $E_s(\lambda)$. The primary advantage of the deployment technique of the instrument in free fall profiling mode is, it provides a straightforward method of making measurements away from the ship at a minimum distance of 20 m by checking the

location of the sun and the sensor should be on the same side to reduce the measurement errors created by the shadow of the ship during deployment. The free-fall descent rate of the instrument is user-adjustable from 0.1 m/sec to 1.0 m/sec (typical) through the use of lead ballast located within the instrument by adding or removing weight as required, with 0.1 to 0.3 m/sec recommended for case-II waters.

The Profiler-II is also equipped with a precision Druck PMP 4000 series pressure sensor which provides accurate depth data (0.04% full-scale typical) and a tilt sensor Clinometer for tilt measurements in two axes (pitch and roll) and provides a linear operating range of $\pm 25^\circ$, with an accuracy of 0.2° . When the instrument is ready to deploy, a pressure tare has been performed with the instrument on deck which provide the actual depth of the profiler. After the pressure tare has been conducted, the instrument is dropped for profiling whereas a pressure tare is required to zero the pressure sensor optical systems to measure depth. The Profiler II is equipped with conductivity and temperature to determine the water temperature over an operating range of -2.5°C to $+40^\circ\text{C}$. The WET Labs ECO FLbb-CD sensor embedded within the Hyperpro-II was used to measure the Chlorophyll concentrations, total particle backscattering at 700nm and CDOM absorption at 460nm. In this study, the in-vivo chlorophyll-*a* fluorescence profiles data using Fluorometer in these coastal waters was collected from surface to 150m of depth and the accuracy of the measurements of chlorophyll concentrations are followed by the ACT protocols.

7.3.2 Water Sample Collection

The *in-situ* water sample data were collected at 21 stations in the cruise dates in coincidence with the OCM-2 satellite pass. Sampling was carried out daily by collecting seawater from 7 depths (0, 5, 15, 25, 30, 50 and 75m) using Niskin water samplers. Filtrations were done immediately, using Whatman GF/F filters and stored -20°C to extract the Chlorophyll pigments by HPLC analysis.

7.4 Data processing methods

There are various techniques to measure chlorophyll, including Spectrophotometry, high performance liquid chromatography (HPLC), Fluorometry and Satellite retrieval. The methodological variability is caused by merging measurements from different instruments, both below surface and above surface, processed with variable procedures.

7.4.1 *In-situ* data processing

The raw radiometric profiles collected using Hyperpro-II were processed using Prosoft 7.7.16 software to extract the radiance parameters collected onboard the vessel by loading all instrument configuration information i.e., the calibration files of the sensors embedded in the instrument and loading the processing parameters by applying dark correction to the data when averaging. In this processing chain we used the multilevel processing i.e., from L1a raw binary data to L4 generated data product and processing was carried out by applying the calibration data to all optical and ancillary sensors for conversion of binary data, by corrections and checks which include pressure tare correction, wavelength sequence, tilt angle for quality control and finally to generate the data product of radiances. In the extraction of chlorophyll concentration profiles of Fluorometer at each depth Morel (2001) model has been used and the SeaBAM and Gordon models for the estimation of surface water chlorophyll concentrations. In order to validate the *in-situ* data with the satellite data the fluorometric measurements of chlorophyll-*a* concentrations were averaged to a subsurface depth of 5m.

7.4.2 High Performance Liquid Chromatography Analysis

Samples were collected in plastic bottles and for the pigment analysis samples were immediately filtered on a GF/F filter (pore size 0.7 μ M) avoiding exposure of the filter paper to direct light and high temperature. The filter paper was stored in liquid nitrogen until for analysis in the laboratory. The frozen filters were immersed in 3 ml 95% acetone (v/v in de ionized water) for extraction using a sonicator probe (5s, 25 μ M) under low light and temperature (4°C) followed by

storage at -20°C for 4h. Pigments Analysis was done by High Performance Liquid Chromatography (or high pressure liquid chromatography) as per the JGOFS protocols 1994. From this the chlorophyll-*a* pigment concentration has been extracted from the samples collected at different locations at different depths. For validation with the *in-situ* measurements the extracted concentrations were averaged to a subsurface depth of 5m and surface measurements were considered for validation with satellite data.

7.5 Results and Analysis

The spatial distribution of chlorophyll-*a* along the transects for the corresponding cruise dates are shown in figure 17 which shows a decrease in the chlorophyll-*a* concentration while moving away from the coast towards the offshore waters of Kakinada and Yanam regions on the corresponding satellites passes. Validation of the chlorophyll algorithms was carried out by comparing chlorophyll-*a* derived from OCM-2 images with *in situ* data collected concurrently (\pm 2hours) and HPLC chlorophyll-*a* data. A total of 33 matching chlorophyll-*a* measurements were considered for comparison of *in-situ* and HPLC data and 10 matching data points were found between 02 and 09 March 2012 for comparison of Satellite measurements with HPLC, *In-situ* data. All the two chlorophyll algorithms produced approximately similar results. In general, they overestimated chlorophyll-*a* at higher concentrations and underestimated it at lower concentrations. When comparing satellite-derived chlorophyll with *in-situ* measured and HPLC chlorophyll data, on 5th and 7th March 2012 data in some parts of the sampling locations were masked out in the processing scheme (i.e., atmospheric correction) become dominant over the bio-optical algorithm.

7.5.1 Comparison of *in-situ* chlorophyll-*a* with OCM-2

As a part of validation the *in-situ* measured chlorophyll-*a* concentration has been compared with satellite derived chlorophyll-*a* during the study period using various chlorophyll-*a* algorithms like OC2 and OC4-V4 (O'Reilley et al., 1998). As mentioned in Table1 of the acquired satellite passes with corresponding cruise dates were used to as input to the SeaDAS processing software

for generation of the chlorophyll images. A scatter plot was made between the *in-situ* measured chlorophyll-*a* concentration and the satellite derived (a) OC2 and (b) OC4) chlorophyll concentration as shown in figure 19. From the scatter plot is for all the sampling points which is not very significant for concentrations greater than 2.0 mg m⁻³ in case of OC2 and >3.0 mg m⁻³ in case of OC4 derived chlorophyll. From this it is clear that there is an under estimation of chlorophyll-*a* concentration in the coastal waters of the OCM-2 data.

7.5.2 Comparison of *in-situ* (radiometer) chlorophyll-*a* with HPLC

Chlorophyll-*a* concentration was measured using HPLC technique for all the stations and for all the depths. The highest concentration of chlorophyll-*a* concentration found was 18 mg m⁻³ in 2007 that increased to 22 and 28 mg m⁻³ in 2008 and 2009 (Acharrya et al., 2012) whereas in this case the high concentrations of chlorophyll-*a* about 7 mg m⁻³ was observed in Kakinada Bay compared to the Godavari estuarine region. However, an attempt is made to compare the chlorophyll-*a* concentration measured from HPLC and *in-situ* measurements. As the radiometric and HPLC measurements of chlorophyll-*a* concentration were averaged to subsurface depth of 5m and showing an increment in the chlorophyll-*a* concentration A very good correlation between these measurements were observed with an R² value of 0.78 as shown in figure 18.

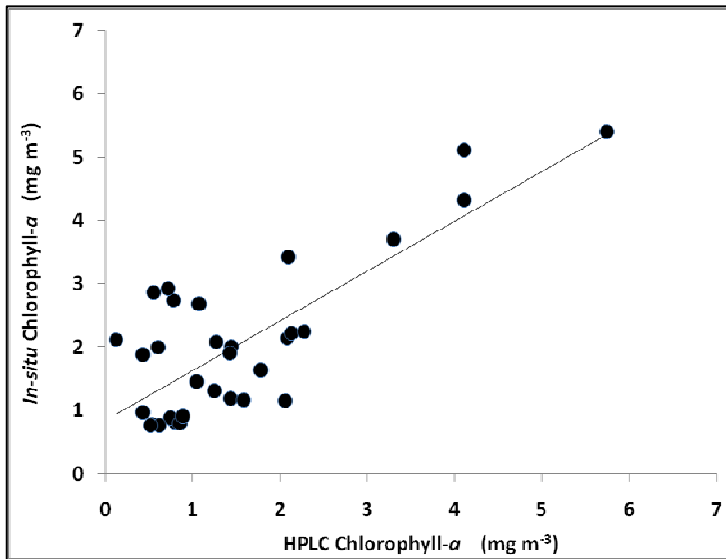


Figure 18: HPLC measured Chlorophyll-*a* concentrations compared with *In-situ* (radiometer) Chlorophyll-*a*

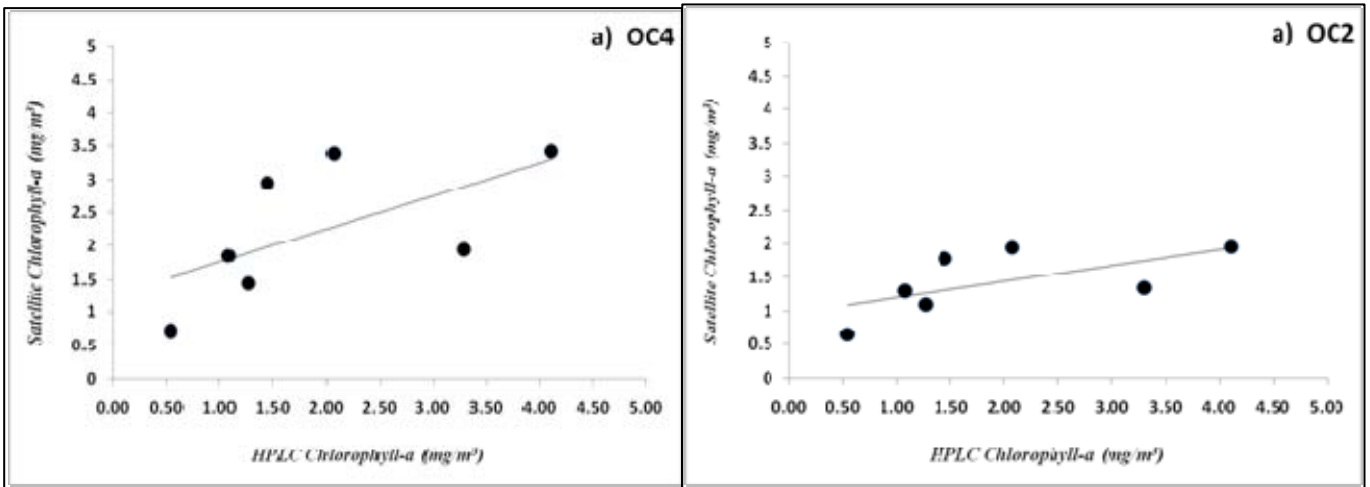


Figure 19: HPLC measured Chlorophyll-a concentrations compared with OCM-2 derived Chlorophyll-a concentrations.

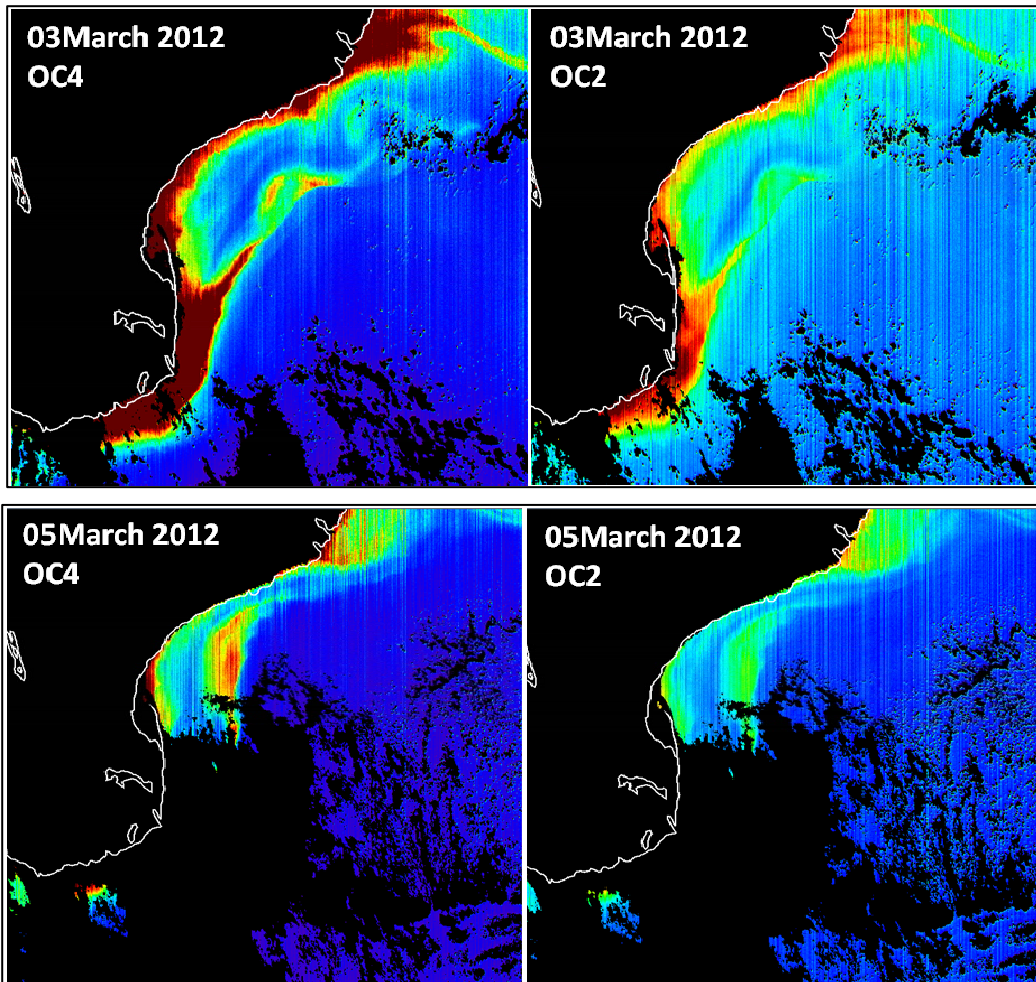
7.5.3 Comparison of HPLC chlorophyll-a with OCM2

Apart from the inter comparison of the *in-situ* measured chlorophyll-*a* concentration with OCM-2 derived chlorophyll concentrations an attempt is made to compare the HPLC measured chlorophyll concentrations with the OCM-2 derived chlorophyll-*a* concentrations as shown in figure 19. From the analysis it is observed that a good correlation with an R^2 value of 0.6 and 0.59 was observed with OC2 and OC4 respectively. The spatial distribution the chlorophyll-*a* concentration during the cruise period processed using OC2 and OC4 algorithms for 3, 5, 7 and 9 March 2012 are shown in figure 20.

7.5.4. Inferences

From this analysis it is observed that the existing global ocean colour algorithms over estimates in the near shore coastal waters as well as estuarine regions of Godavari. In this optically complex waters near the estuarine waters if the chlorophyll-*a* concentration is greater than ~2.5 mg m⁻³ the current global ocean colour algorithms fail. If we consider a small local / regional geographical province and then apply these algorithms for a particular province these algorithms

works better rather than taking the total basin a whole for validating the algorithms. Where not only the chlorophyll concentration plays a major role like the sediment re-suspension, pigment and the shell structure which is being formed by calcification. The costal system is more optically complex because of short-term coastal upwelling, enhancement of nutrients because of river run-off and anthropogenic activity and biological process like nitrification, de-nitrification, carbonate system etc which has direct bearing with phytoplankton growth and their pigment characterization. Besides the area is dominated by unicellular diatoms basically contains silica. Hence the costal process becomes more complex in terms of bio-geo chemical behavior. Hence retrieval of chlorophyll becomes erroneous in its quantification. Further refinement of the atmospheric correction is needed for OCM-2 to attain its goal of accuracy for chlorophyll retrieval in the coastal waters. This requires specific, suitable regional bio-optical algorithms such as fluorescence based and inherent optical properties (IOPs) based algorithms to overcome this problem.



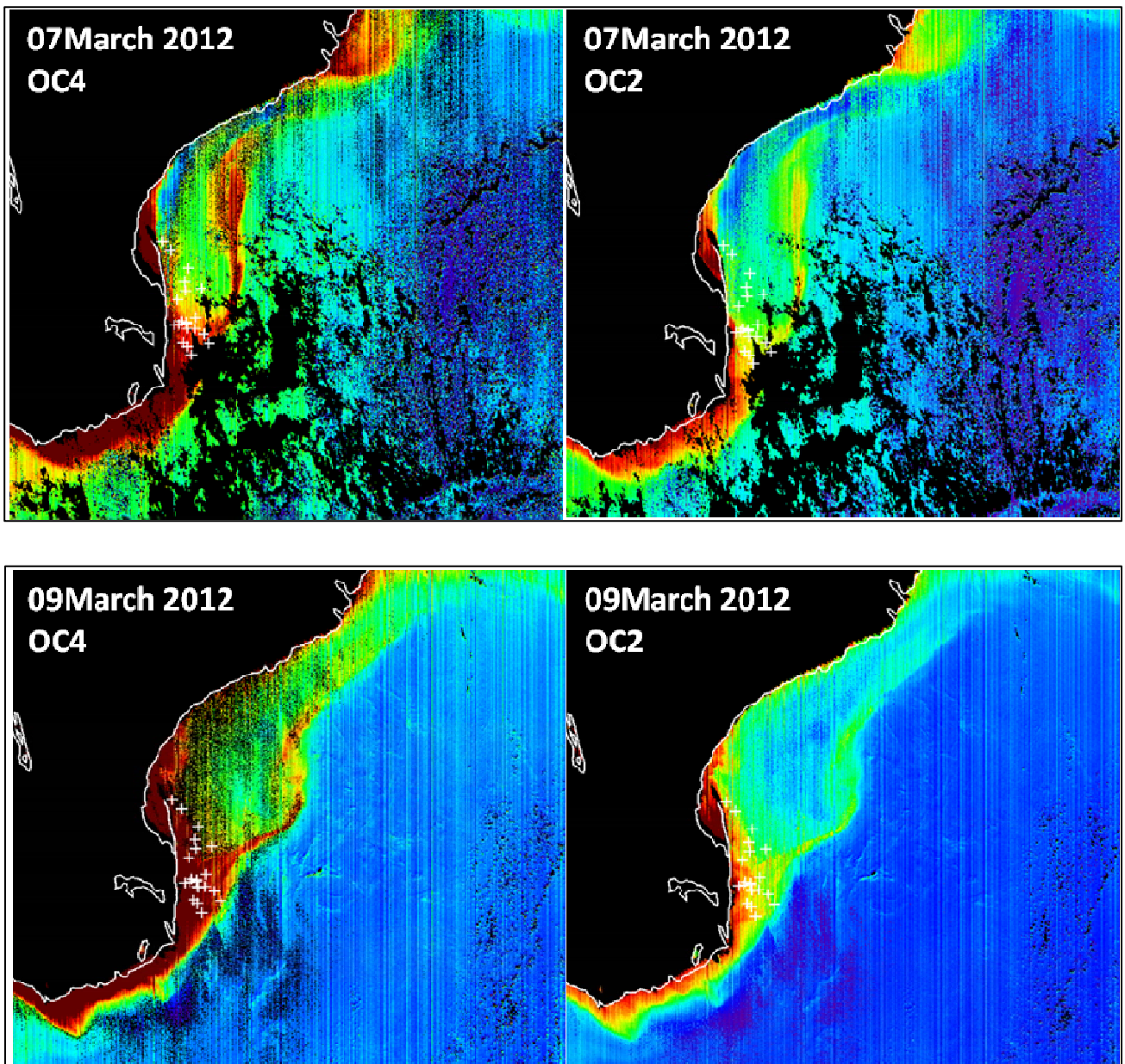


Figure 20: Spatial distribution of Chlorophyll-a derived from OCM-2 on corresponding cruise dates

8. Conclusions

From this study we conclude that, Oceansat-2 Ocean Colour monitor being a global mission needs globally accepted geophysical data products. for this purpose we need to process OCM-2 data with uniform bio-optical algorithms, uniform atmospheric correction procesured including flags, masks and other ancillary information which is globally accepted for the other Ocean Colour missions for generating the geophysical data products. Hence, we took an initiative to process OCM-2 data using the global ocean colour data processing software for generating the geophysical parameters. Apart from this the products generated by OCM-2 needs to be validated in both Indian as well as global waters for wide acceptance of OCM-2 products. Initially we validated OCM-2 data with three coastal cruises conducted in the Bay of Bengal in 2012. Further validation of the OCM-2 products in the global waters needs to be taken up. The final products of chlorophyll-a distribution over the north Indian Ocean as well in the global oceans are shown in Annexure I to V for the year 2012.

9. Acknowledgements

This work has been carried out as a part of ISRO-IGBP, NCP project of National Remote Sensing Centre, ISRO. The *in-situ* observations were measured in collaboration with NIO-RC, Visakhapatnam, CSBOB, Andhra University, Department of Zoology, Andhra University, ICMAM, MoES, Chennai. All the authors would like to thank the respective Institutions for their inconsistent support for making this cruise a grand success. We acknowledge SeaDAS data processing software team for providing the software.

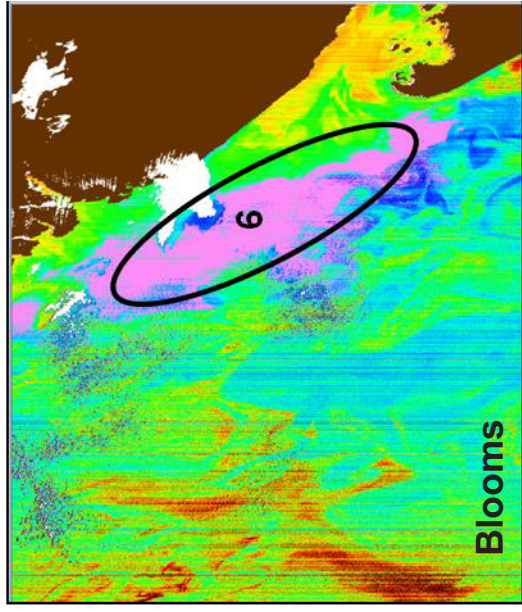
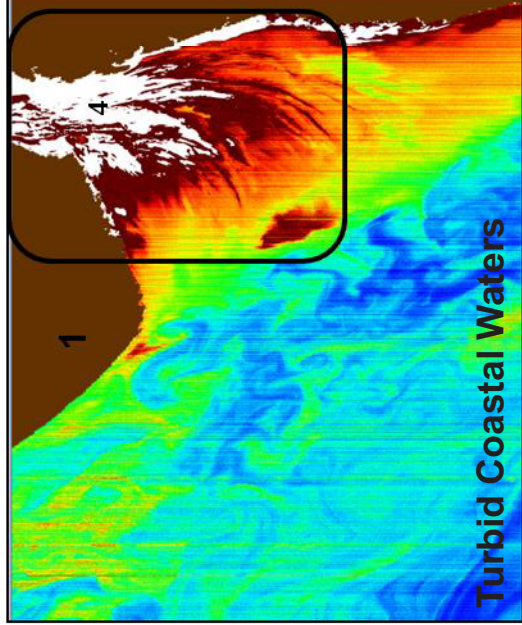
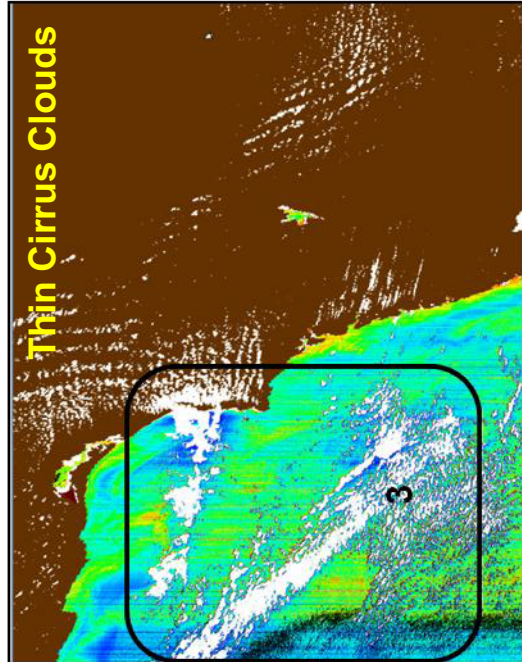
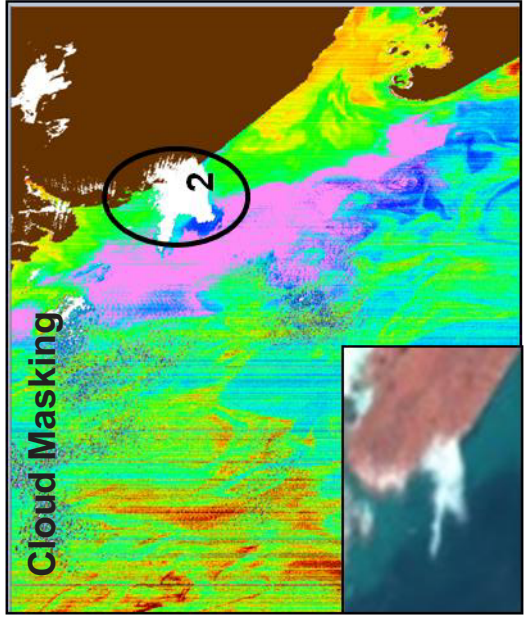
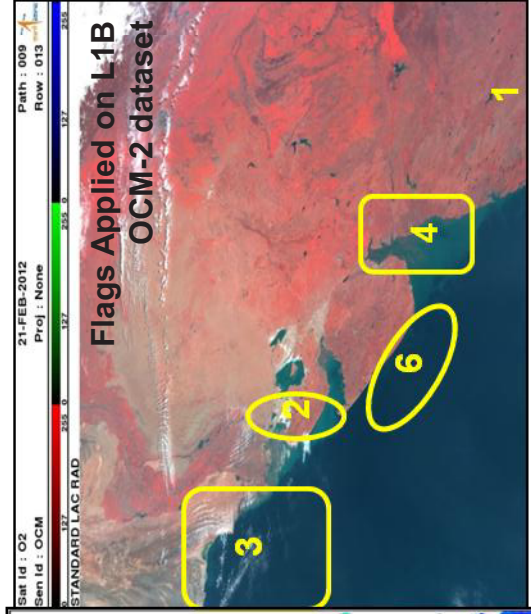
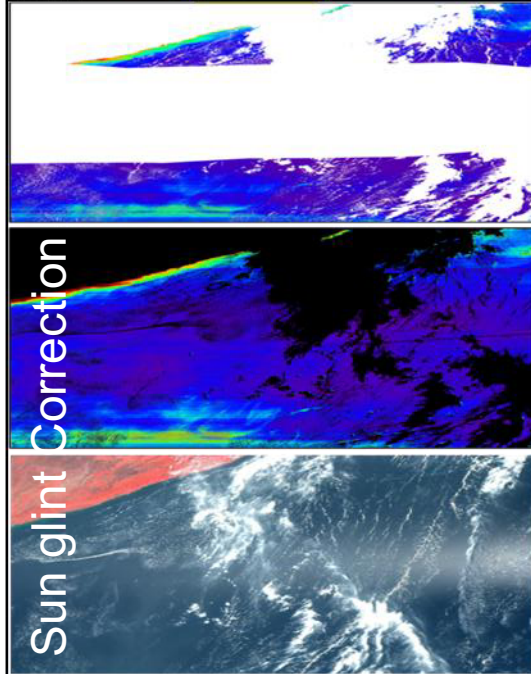
10. References

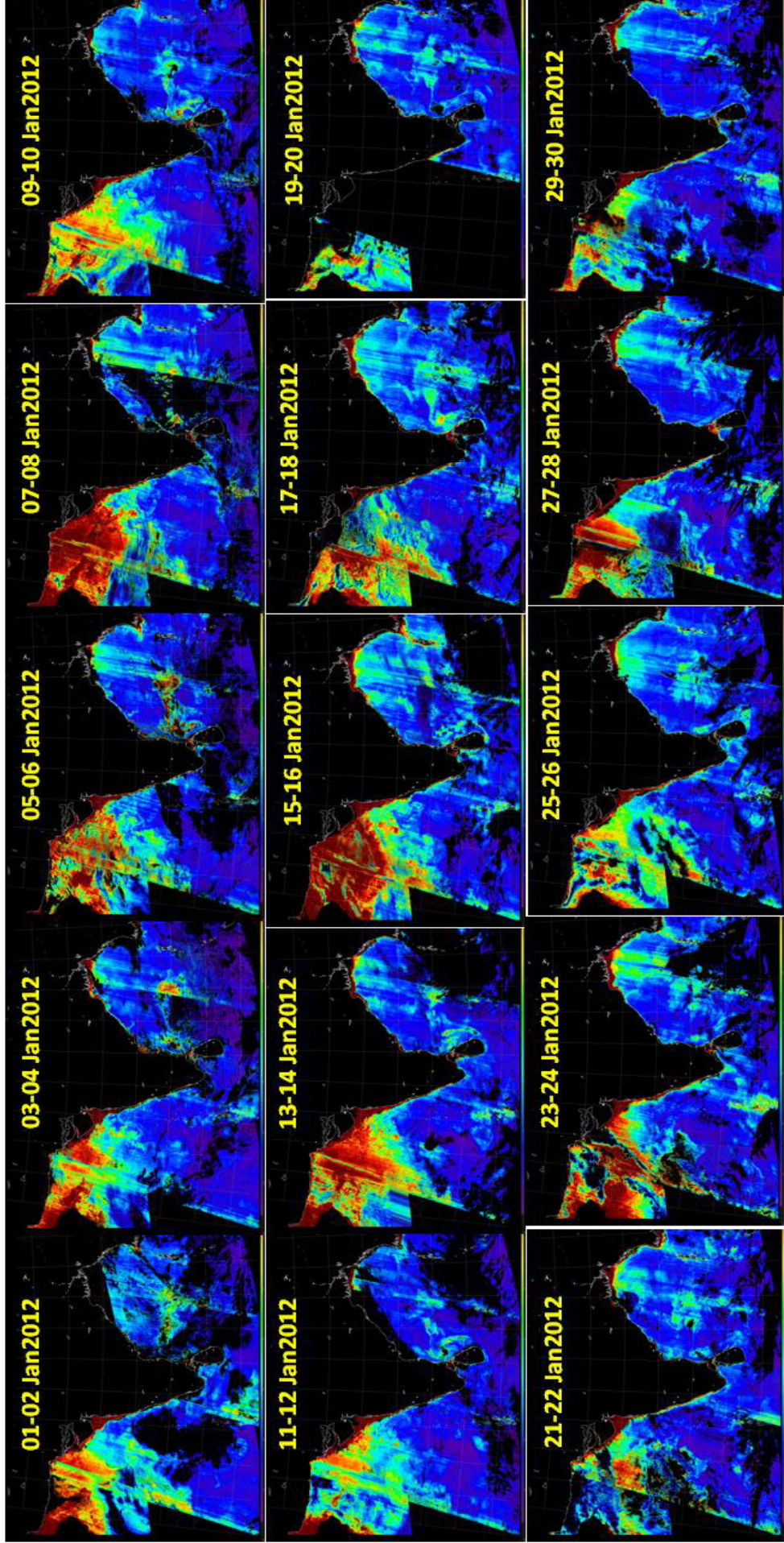
1. H. R. Gordon, and M. Wang, "Retrieval of water-leaving radiance and aerosol optical thickness over the oceans with SeaWiFS: a preliminary algorithm," *Appl. Opt.* **33**(3), 443–452 (1994).

2. D. A. Siegel, M. Wang, S. Maritorena, and W. Robinson, "Atmospheric correction of satellite ocean color imagery: the black pixel assumption," *Appl. Opt.* **39**(21), 3582–3591 (2000).
3. C. R. McClain, E. Ainsworth, R. Barnes, R. Eplee, Jr., F. Patt, W. Robinson, M. Wang, and S. W. Bailey, "SeaWiFS Postlaunch Calibration and Validation Analyses, Part 1," NASA Tech. Memo. 206892, National Aeronautics and Space Administration, Goddard Space Flight Center, Greenbelt, MD (2000).
4. A. Morel, "Optical modeling of the upper ocean in relation to its biogenous matter content (case 1 waters)," *J. Geophys. Res.* **93**(C9), 10749–10768 (1988).
5. R. P. Stumpf, R. A. Arnone, J. R. W. Gould, P. M. Martinolich, and V. ansibrahmanakul, "A partially coupled ocean-atmosphere model for retrieval of water-leaving radiance from SeaWiFS in coastal waters," in Patt, F.S., et al., 2003: *Algorithm Updates for the Fourth SeaWiFS Data Reprocessing*. NASA Tech. Memo. 206892, National Aeronautics and Space Administration, Goddard Space Flight Center, Greenbelt, MD (2003).
6. H. R. Gordon, O. B. Brown, R. H. Evans, J. W. Brown, R. C. Smith, K. S. Baker, and D. K. Clark, "A semi analytic radiance model of ocean color," *J. Geophys. Res.* **93**(D9), 10909–10924 (1988).
7. R. W. Gould, Jr., R. A. Arnone, and P. M. Martinolich, "Spectral dependence of the scattering coefficient in case 1 and case 2 waters," *Appl. Opt.* **38**(12), 2377–2383 (1999).
8. Z. Lee, R. A. Arnone, C. Hu, P. J. Werdell, and B. Lubac, "Uncertainties of optical parameters and their propagations in an analytical ocean color inversion algorithm," *Appl. Opt.* **49**(3), 369–381 (2010).
9. Prakash Chauhan, Mannil Mohan, and Shailesh Nayak, 'Comparative analysis of Ocean Colour Measurements of IRS-P4 OCM and SeaWiFS in the Arabian Sea', *Geoscience and Remote Sensing Letters*, vol. 41, No 4, April 2003.
10. O'Reilly, J. E., S. Maritonen, B. G. Mitchell, D. A. Siegel, K. L. Carder, S. A. Graver, M. Kahru & C. R. McClain, 1998. Ocean color chlorophyll algorithms for SeaWiFS. *Journal of Geophysics* 103: 24937–24963.
11. T. Acharyya, V.V.S.S. Sarma, B. Sridevi, V. Venkataramana, M.D. Bharathi, S.A. Naidu, B.S.K. Kumar, V.R. Prasad, D. Bandopadhyay, N.P.C. Reddy, M.D. Kumar, "Reduced river discharge intensifies phytoplankton bloom in Godavari estuary, India", *Marine Chemistry* 132-133(2012) 15-22.

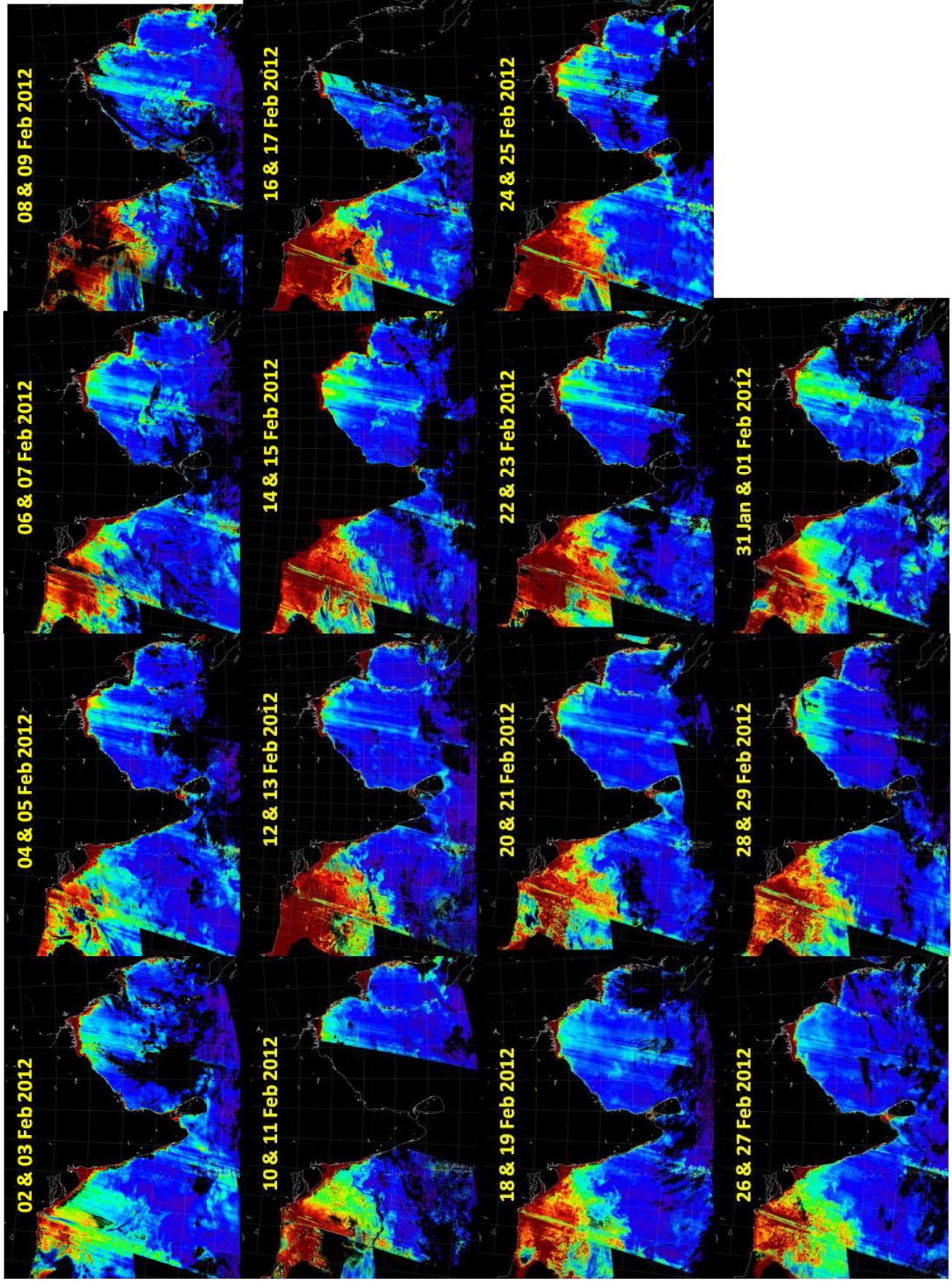
12. Andre Morel and Stepane Maritorena, 'Bio-optical properties of Oceanic waters: A reappraisal'; Journal of Geophysical Research Volume 106, No. C4, pp. 7163-7180, April 2001.
13. <http://seadas.gsfc.nasa.gov>
14. IOCCG report 2, "Status and plans for Satellite Ocean-Colour Missions: Considerations for Complementary Missions" 1999 edited by James A. Yoder.
15. IOCCG report 1, "Minimum Requirements for an Operational, Ocean-Colour Sensor for the Open Ocean" 1998, Chaired by Andre Morel.
16. Pope R.M., and Fry E.S. "Absorption Spectrum (380-700 nm) of Pure Water. II. Integrating Cavity Measurements" Applied Optics, Vol. 36, No. 33, 1997.
17. Bailey, S.W., Bryan A. Franz and P.J. Werdell, "Estimation of Near Infra red Water leaving Reflectance for Satellite Ocean Colour Data Processing" Optics Express, Vol. 18, No. 7, 2010.
18. Andre Morel, 'Optical Modeling of the Upper Ocean in Relation to Its Biogenous Matter Content'; Journal of Geophysical Research, Vol. 93 No. C9, 1998, pp. 10749-10768.
19. A. Morel, D. Antoine, B. Gentili, "Bi-directional reflectance of Oceanic Waters accounting for Raman Emission and Varying particle Scattering Phase Function" Applied Optics, 41 (30), 2002, pp. 6289-6306.

FLAGS & MASKS used for Level1 –Level2 processing

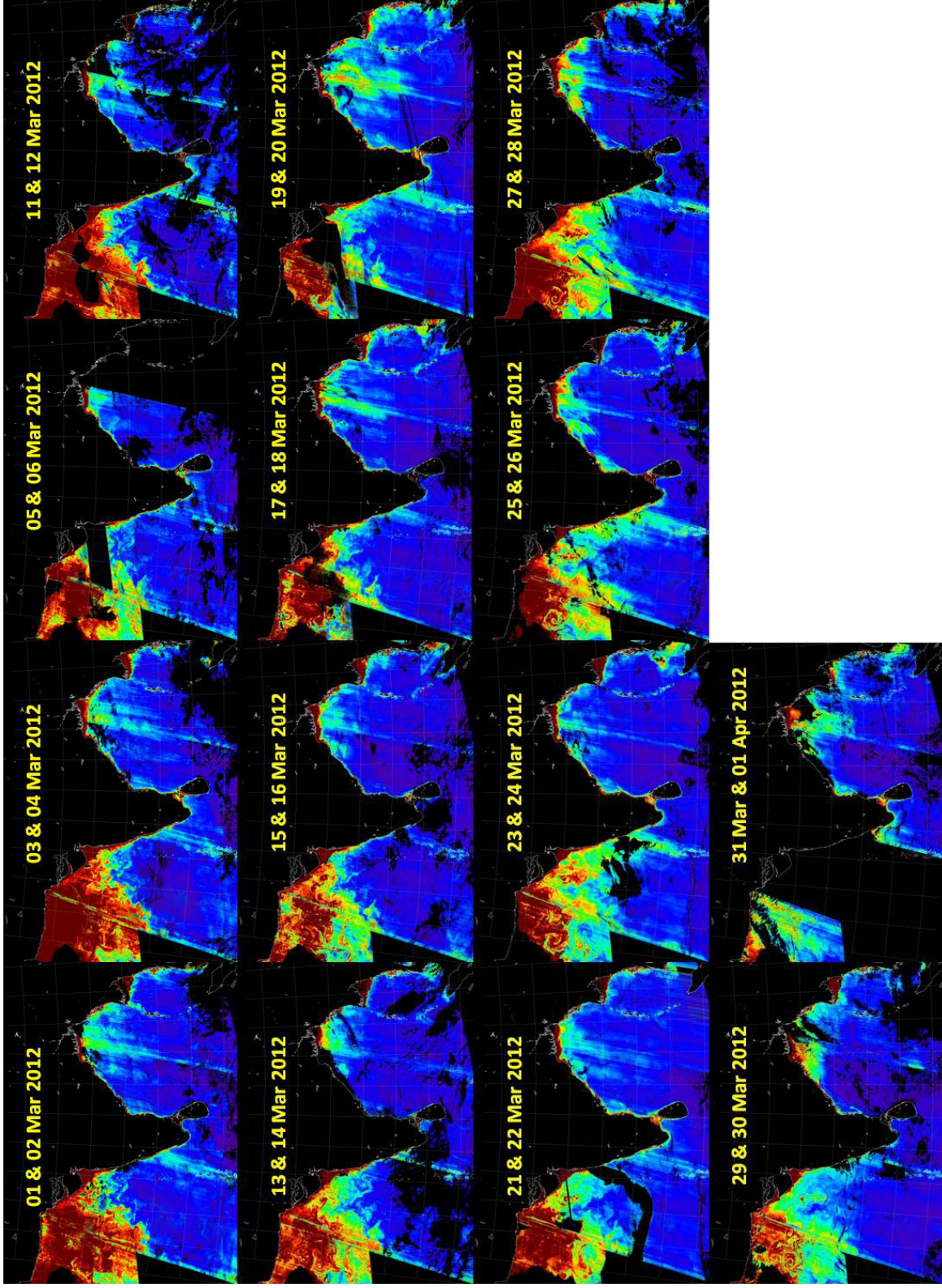




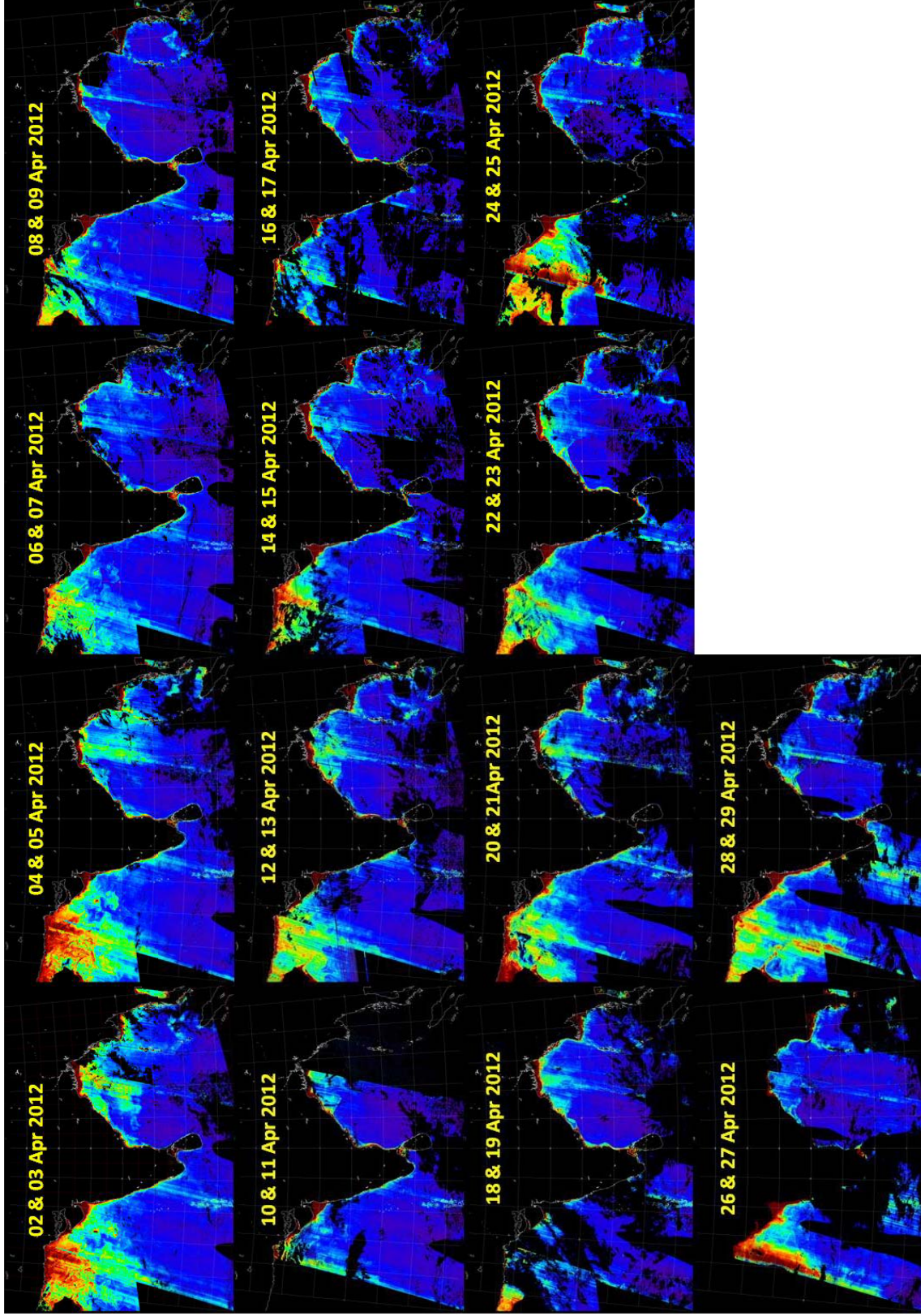
2-day composites of Chlorophyll-a January 2012



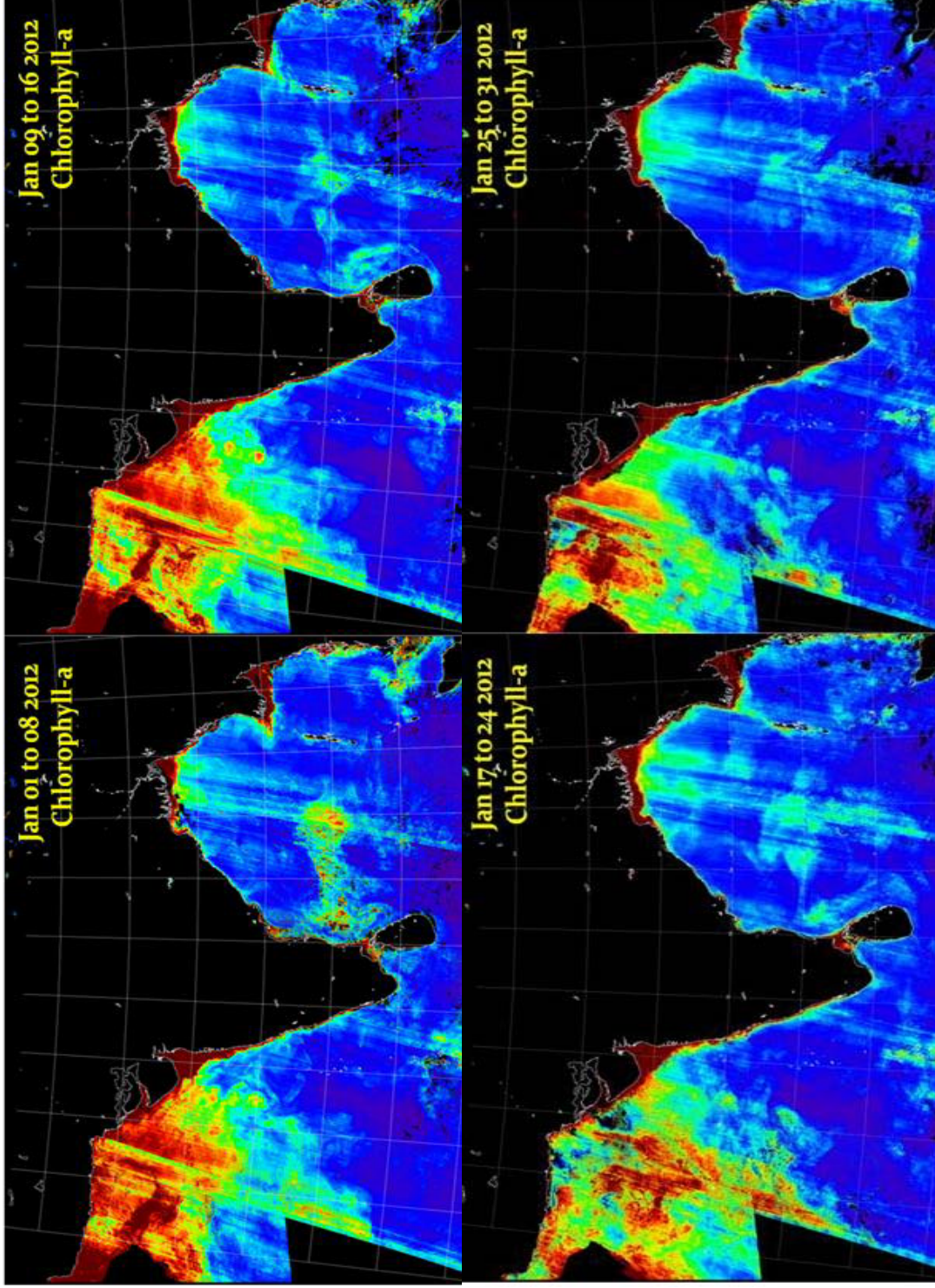
2-day composites of Chlorophyll-a February 2012



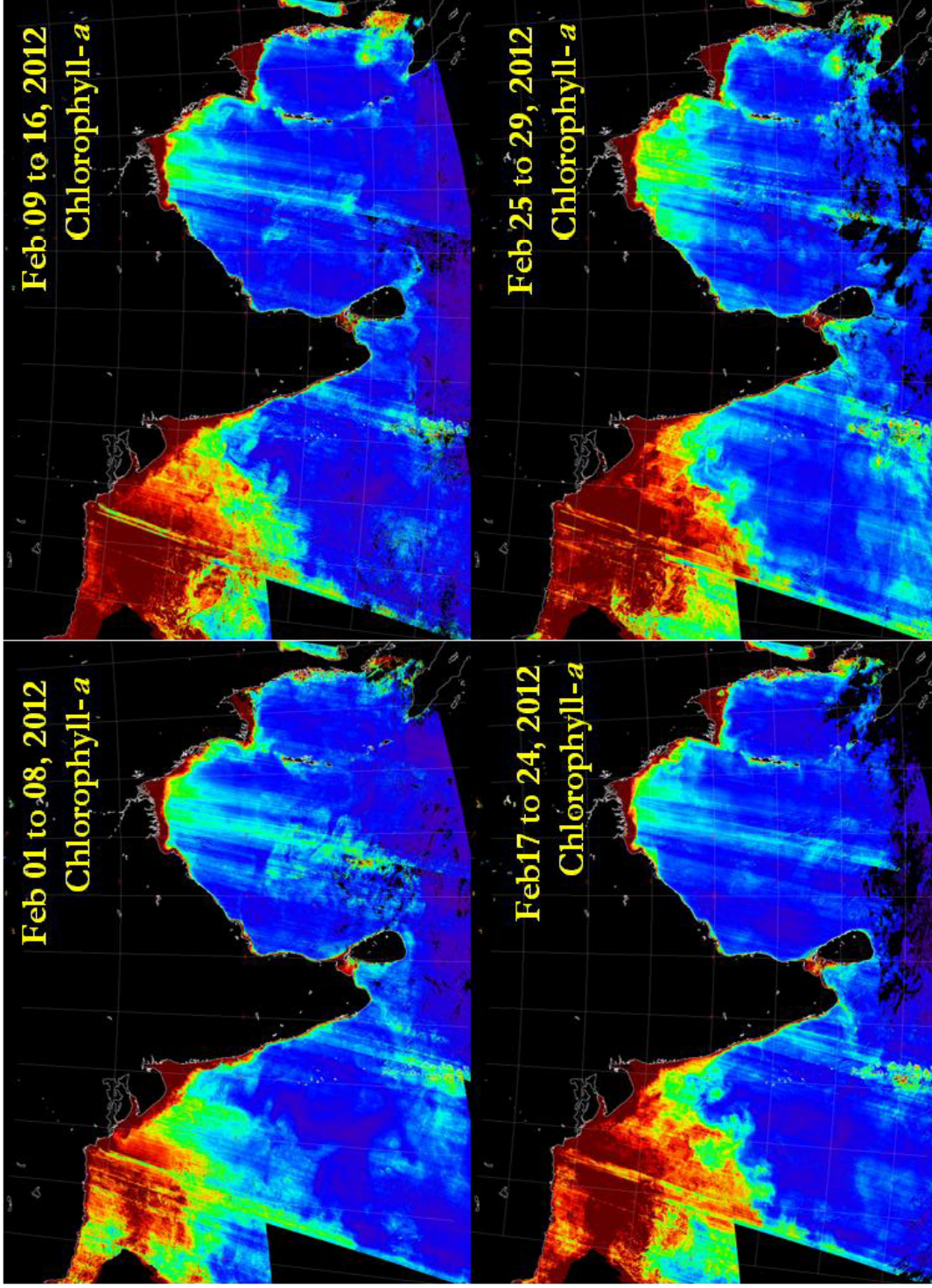
2-day composites of Chlorophyll-a March 2012



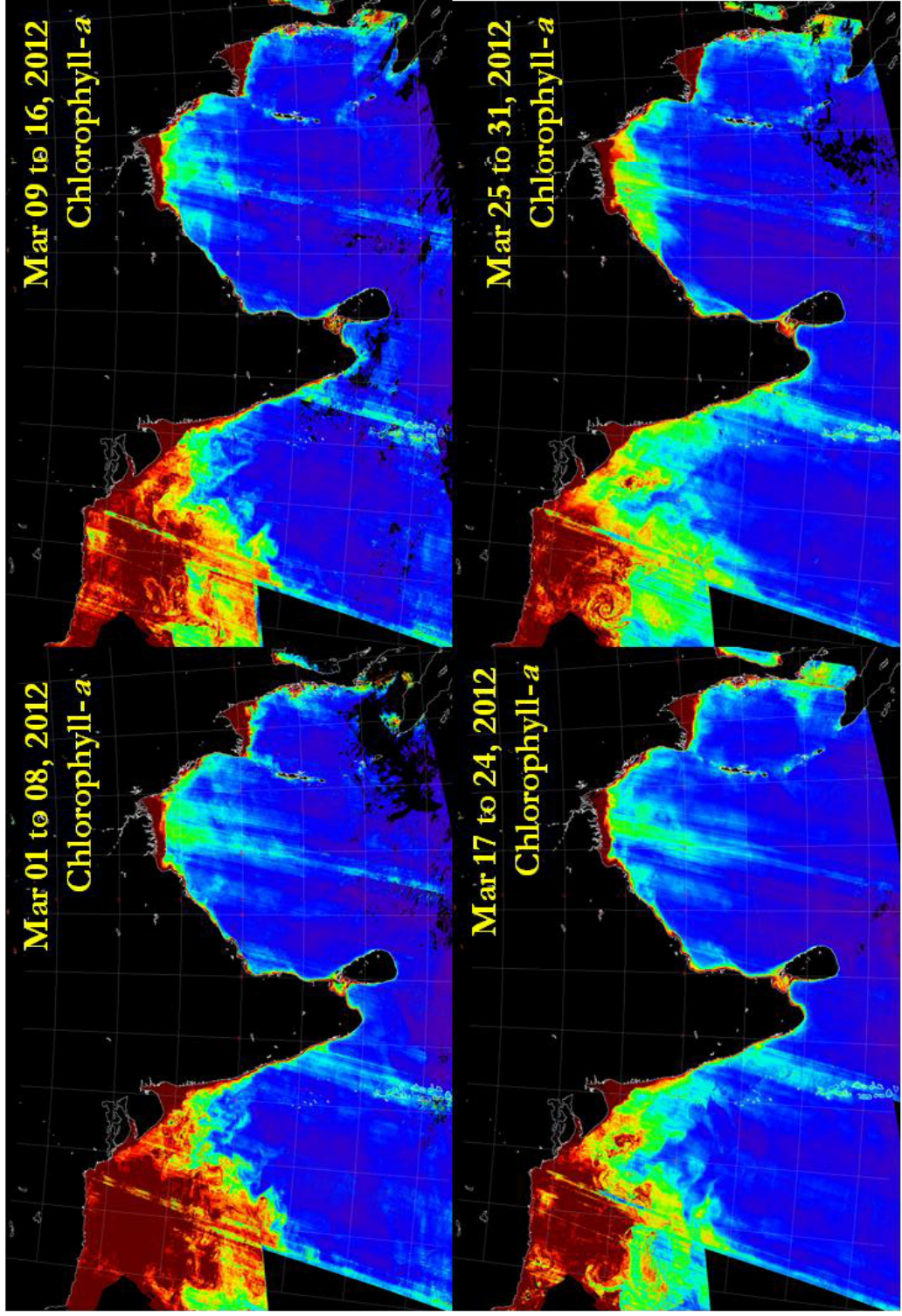
2-day composites of Chlorophyll-a April 2012



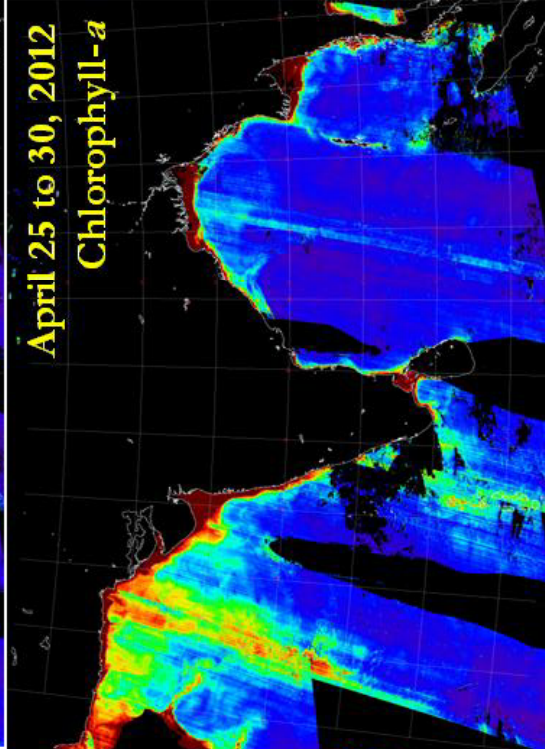
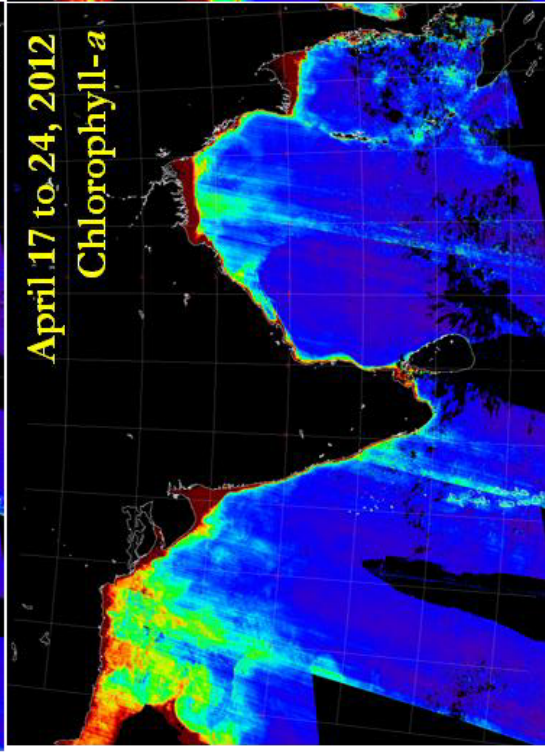
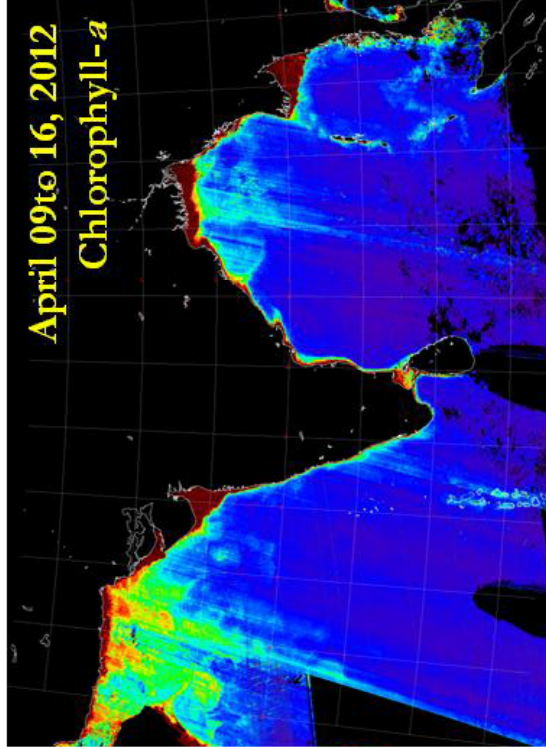
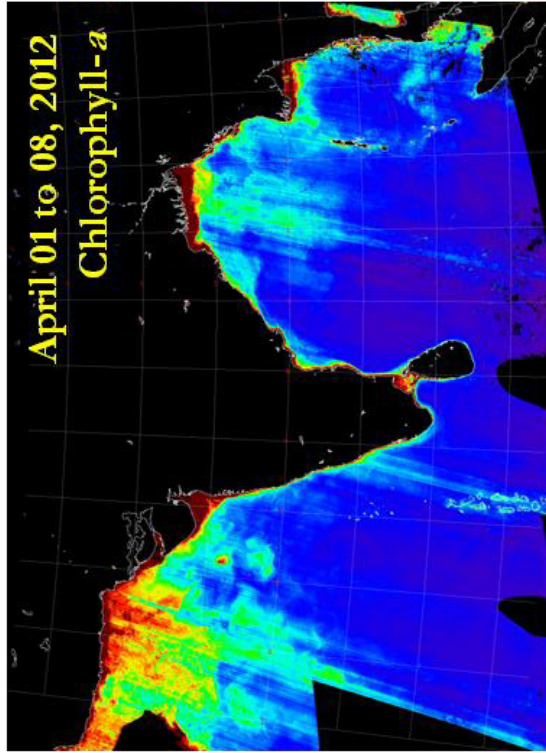
8-day Binned product of Chlorophyll-a January 2012



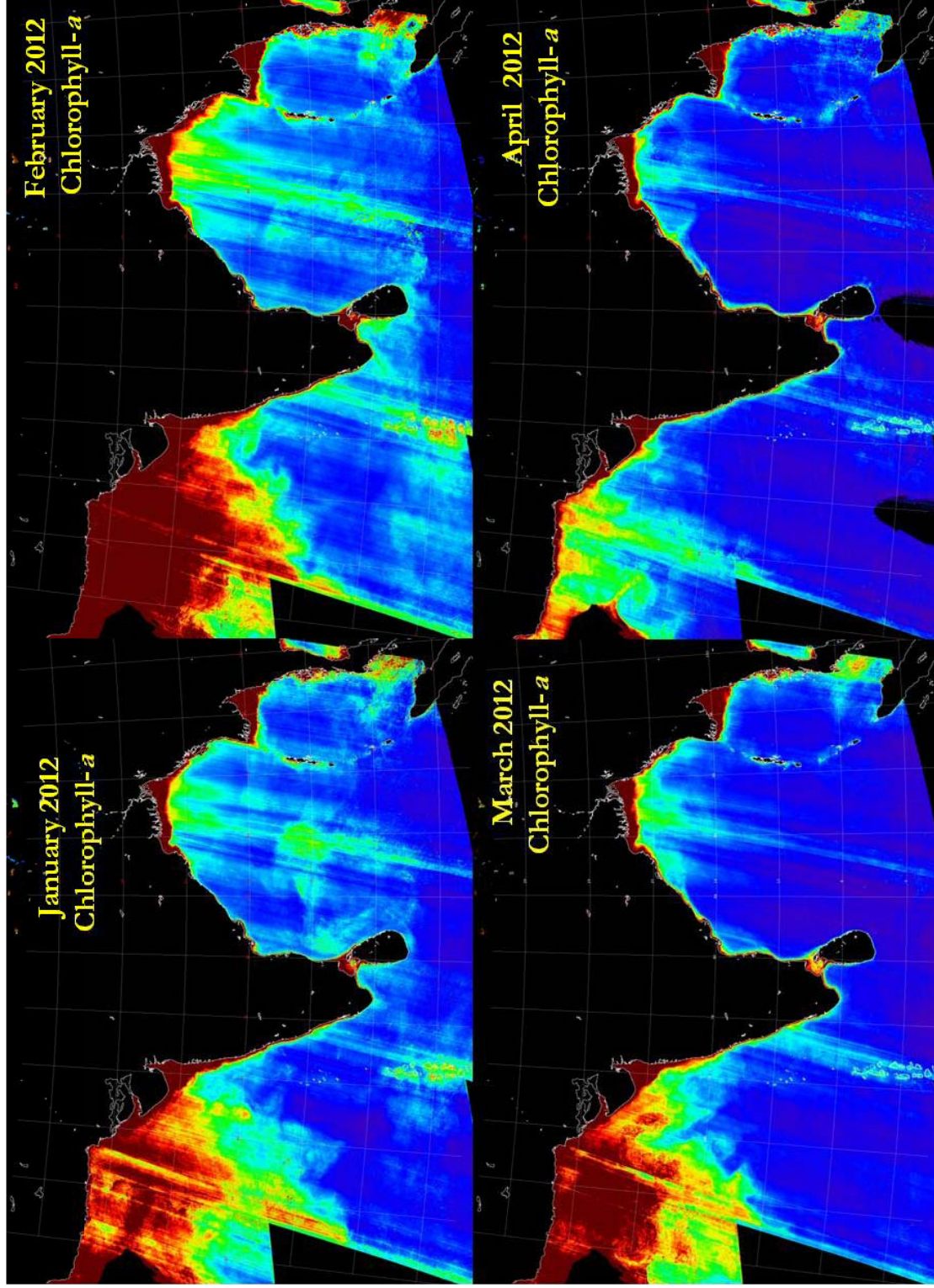
8-day Binned product of Chlorophyll-a February 2012



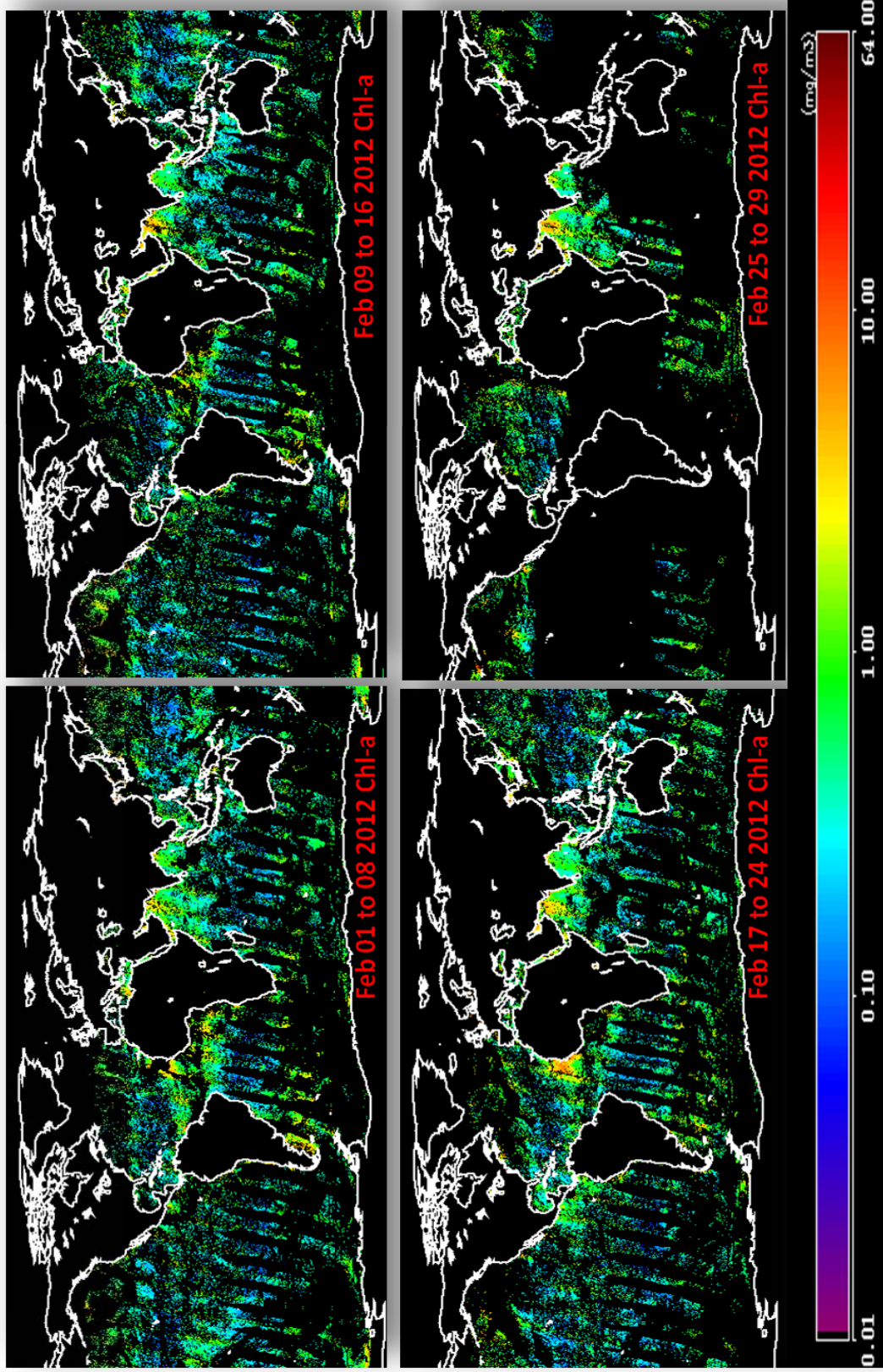
8-day Binned product of Chlorophyll-*a* March 2012



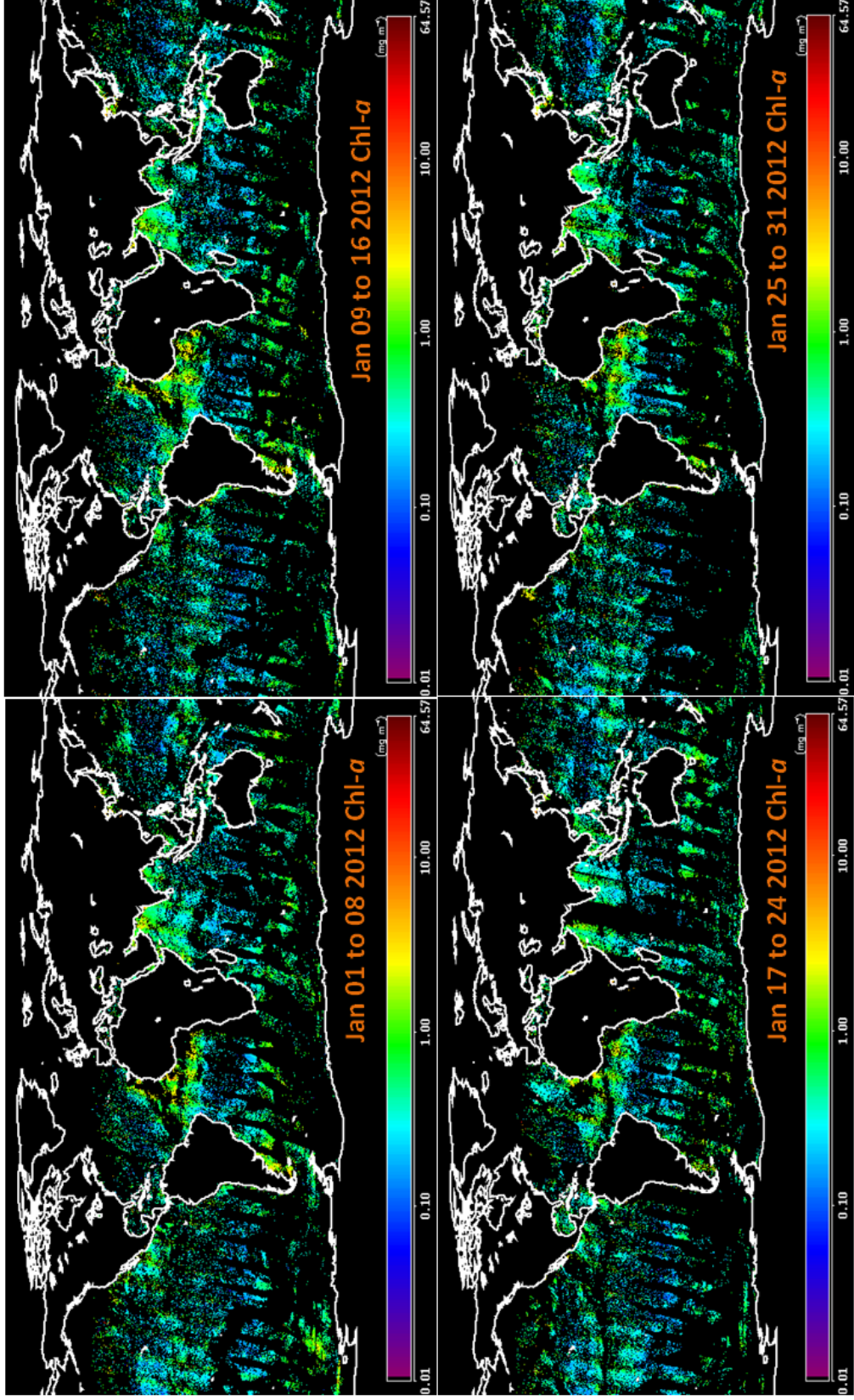
8-day Binned product of Chlorophyll-a April 2012



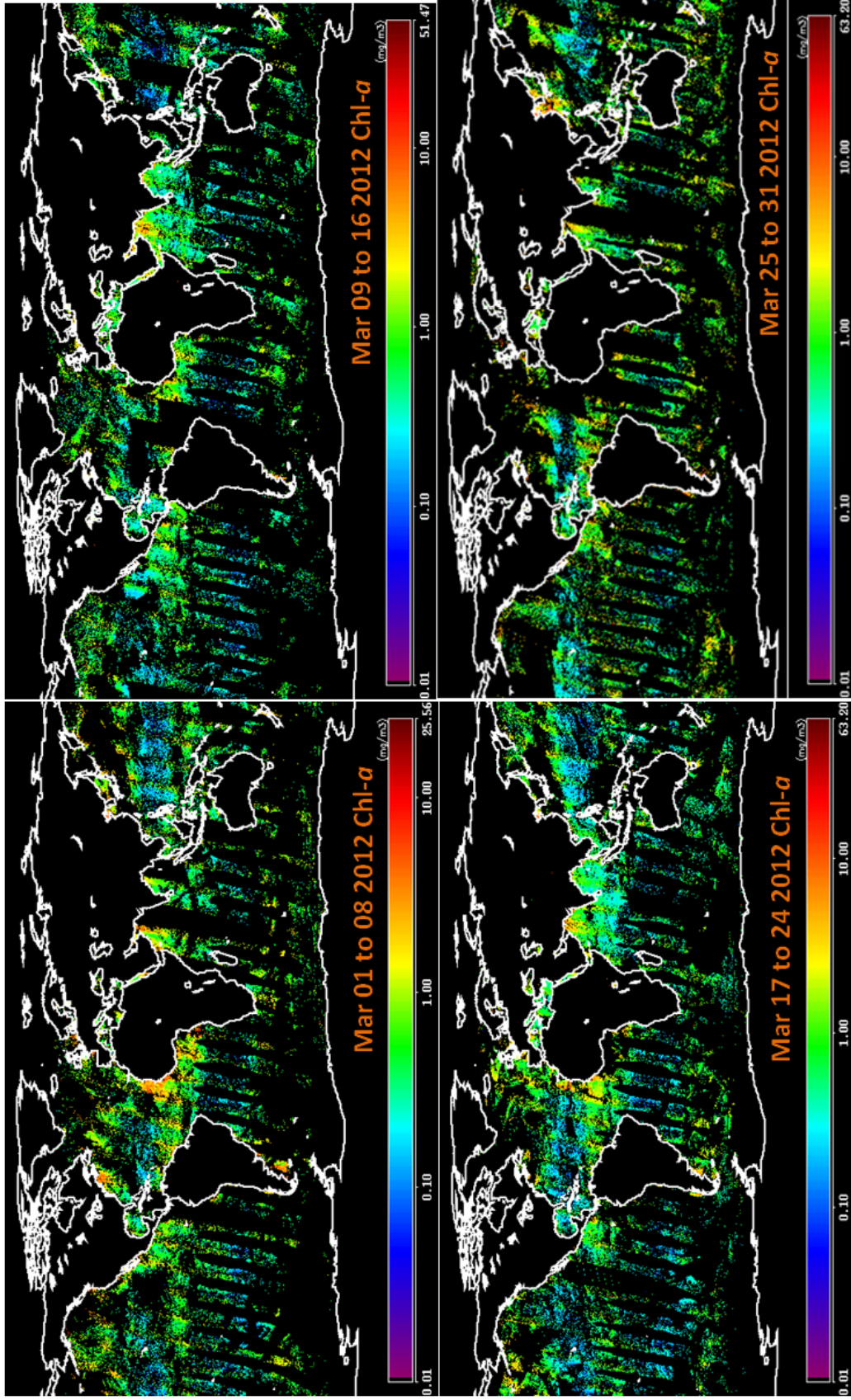
Monthly Binned product of Chlorophyll-a (Jan-Apr) 2012



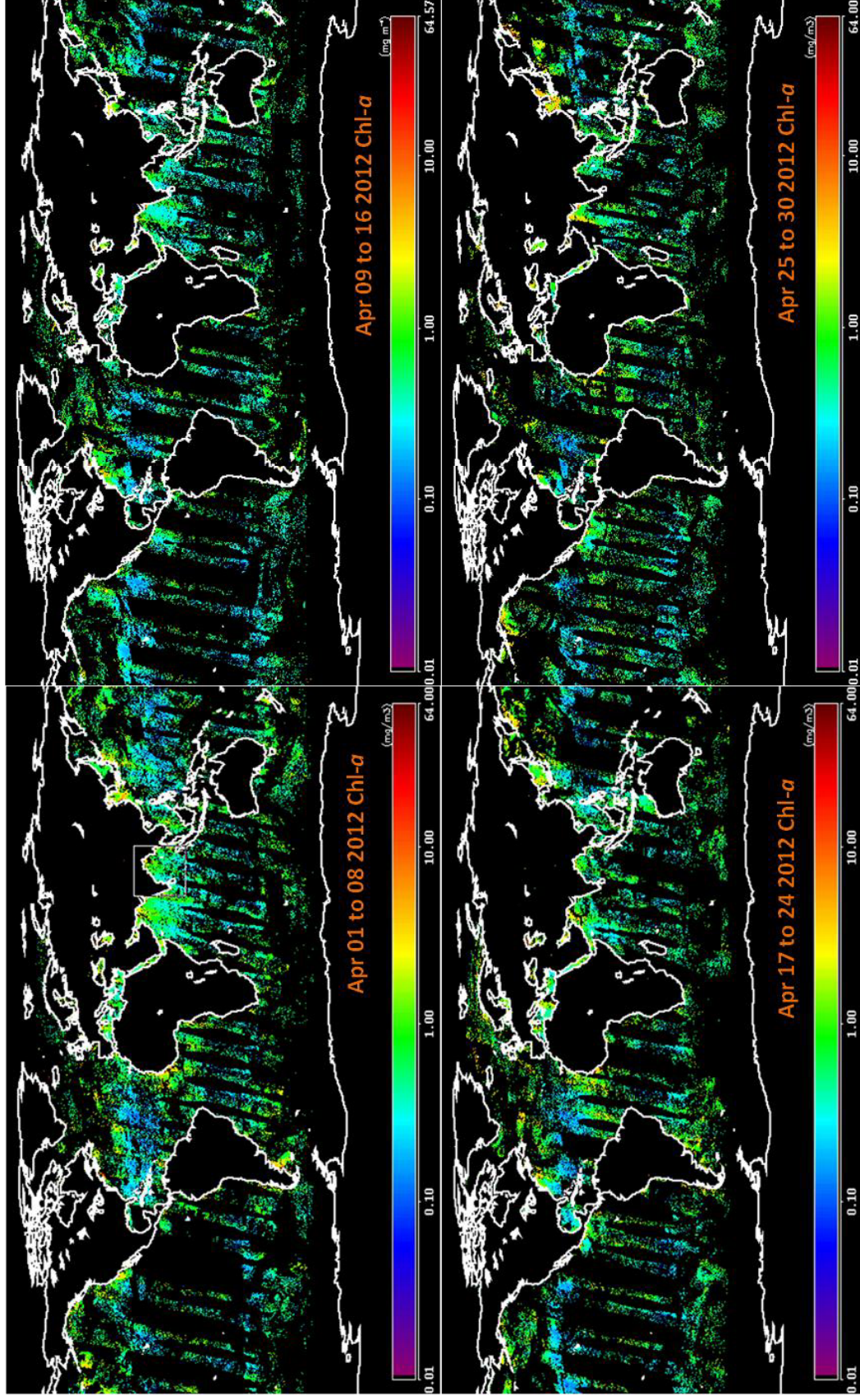
8-day Binned Global Chlorophyll-a product February 2012



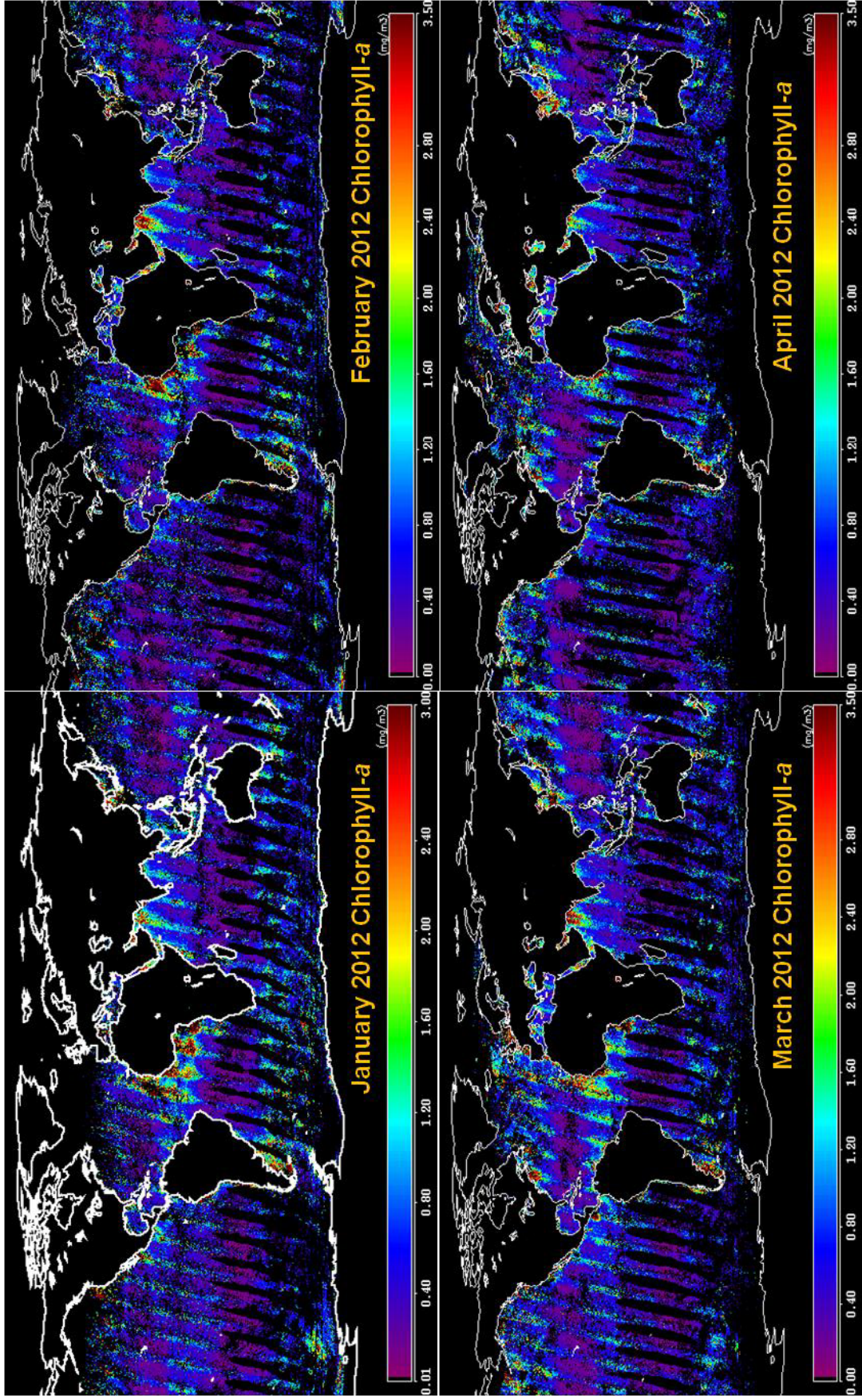
8-day Binned Global Chlorophyll-a product January 2012



8-day Binned Global Chlorophyll-a product March 2012



8-day Binned Global Chlorophyll-a product April 2012



Monthly Binned Global Chlorophyll-a product (Jan-Apr) 2012